Bioactive Materials 5 (2020) 584–601

Contents lists available at ScienceDirect

Bioactive Materials

journal homepage: http://www.keaipublishing.com/biomat

Engineered three-dimensional scaffolds for enhanced bone regeneration in osteonecrosis

Tongtong Zhu[a,b], Yutao Cui[c], Mingran Zhang[a,b], Duoyi Zhao[b], Guangyao Liu[a,*], Jianxun Ding[b]

[a] Department of Orthopedics, China-Japan Union Hospital of Jilin University, 126 Xiantai Street, Changchun, 130033, PR China
[b] Key Laboratory of Polymer Ecomaterials, Changchun Institute of Applied Chemistry, Chinese Academy of Sciences, 5625 Renmin Street, Changchun, 130022, PR China
[c] Department of Orthopedics, The Second Hospital of Jilin University, 218 Ziqiang Road, Changchun, 130041, PR China

ARTICLE INFO

Keywords:
Three-dimensional scaffold
Functionalization
Bone regeneration
Bone tissue engineering
Osteonecrosis therapy

ABSTRACT

Osteonecrosis, which is typically induced by trauma, glucocorticoid abuse, or alcoholism, is one of the most severe diseases in clinical orthopedics. Osteonecrosis often leads to joint destruction, and arthroplasty is eventually required. Enhancement of bone regeneration is a critical management strategy employed in osteonecrosis therapy. Bone tissue engineering based on engineered three-dimensional (3D) scaffolds with appropriate architecture and osteoconductive activity, alone or functionalized with bioactive factors, have been developed to enhance bone regeneration in osteonecrosis. In this review, we elaborate on the ideal properties of 3D scaffolds for enhanced bone regeneration in osteonecrosis, including biocompatibility, degradability, porosity, and mechanical performance. In addition, we summarize the development of 3D scaffolds alone or functionalized with bioactive factors for accelerating bone regeneration in osteonecrosis and discuss their prospects for translation to clinical practice.

1. Introduction

Osteonecrosis, a debilitating disease, also known as ischemic necrosis and avascular necrosis of bone [1,2], exhibits rapid progression and is challenging to diagnose early [3]. Many factors are known to cause osteonecrosis, such as trauma [4,5], glucocorticoid therapy [6,7], alcoholism [8], decompression sickness [9], hyperlipidemia [10], and Gaucher disease [11]. The pathogenesis of osteonecrosis remains controversial [12], and possible pathogenic processes include osteogenic impairment, an imbalance between osteogenic and adipogenic differentiation, oxidative stress, intramedullary pressure changes, fat embolization, and so forth [13–17].

Insufficient blood supply to bones and bone marrow cells reduces bone cell activity and further leads to bone destruction [18]. Therefore, osteonecrosis inevitably results in the progressive collapse of the joints and subsequent arthritis always, for which arthroplasty is ultimately required [19,20]. The main underlying reason is that bone regeneration is hampered in the harsh necrotic microenvironment [21]. Alternative therapeutic strategies include non-surgical as well as surgical managements. Some non-surgical management techniques, such as cell therapy [22–24], growth factor therapy [17,25], cytokine therapy [26], hormone therapy [27,28], and pharmacologic therapy [14,29,30], have shown varying levels of efficacies. However, this management also has apparent disadvantages when administered systemically or *via* local infusion. Systemic administration results in low concentrations at the necrotic area and causes side effects, local infusion of biological agents is also associated with problems, such as leakage, loss of bioactivity, and initial burst release [31–33]. Surgical management often requires bone grafting. Autografts and allografts are highly effective in enhancing bone regeneration in osteonecrosis. However, the grafts are associated with the risk of numerous complications, such as limited bone mass, donor site complications, infection, and immune rejection, which limit their clinical applications [34–37].

Following advances in material and biological sciences, many new insights into the potential applications of biomaterials to optimize bone regeneration in osteonecrosis, with prospects for fulfilling clinical requirements, are proposed. Several studies have demonstrated the advantages of engineered three-dimensional (3D) scaffold-mediated therapy in enhancing bone regeneration during osteonecrosis [38–40]. The 3D structure of the scaffolds mimics the natural microenvironment and provides living space for cells [41,42], their porosity promotes recovery of blood supply and bone ingrowth, and their mechanical performance compensates for the insufficient support provided by the subchondral bone. Furthermore, the use of bioactive factors in

Peer review under responsibility of KeAi Communications Co., Ltd.
* Corresponding author.
E-mail address: gyliu@jlu.edu.cn (G. Liu).

https://doi.org/10.1016/j.bioactmat.2020.04.008
Received 26 February 2020; Received in revised form 11 April 2020; Accepted 11 April 2020
Available online 17 April 2020

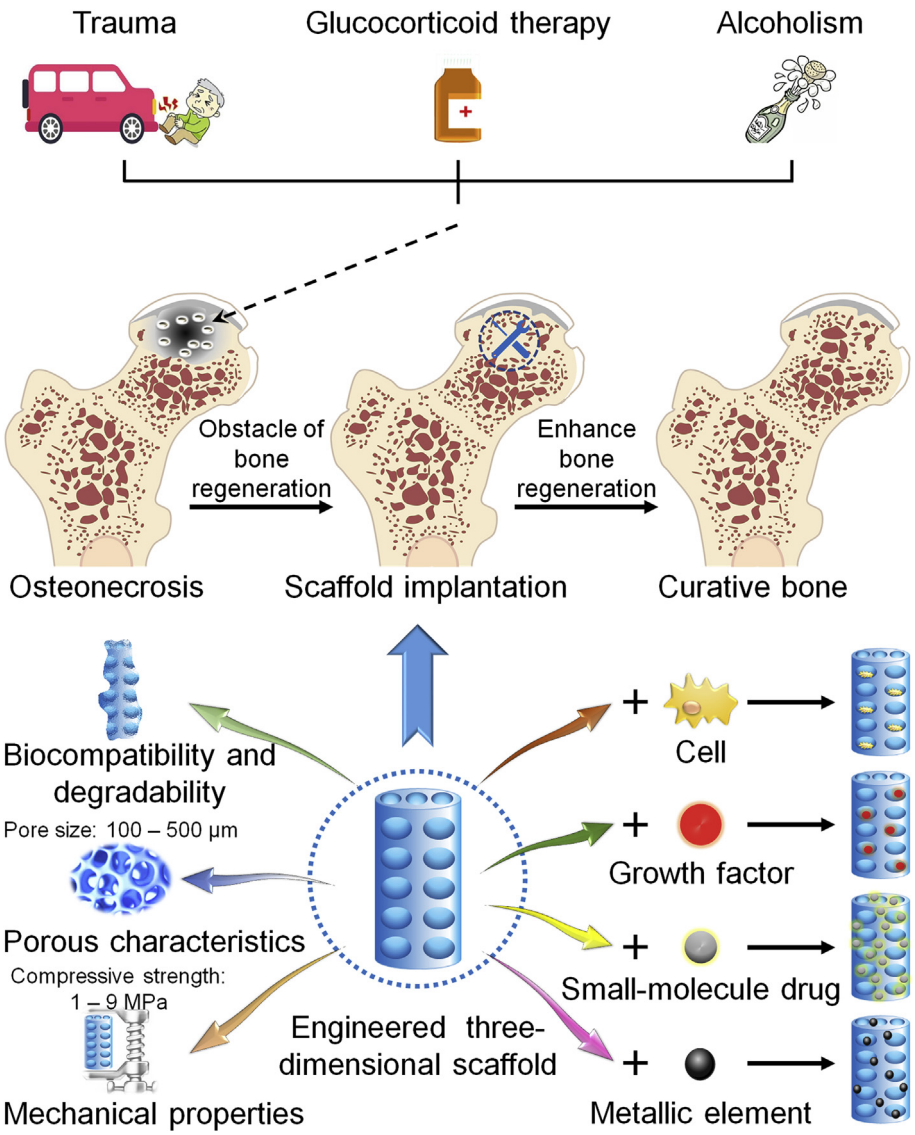

Scheme 1. Engineered 3D scaffold for enhanced bone regeneration in osteonecrosis.

combination with engineered 3D scaffolds makes it possible to limit the decrease in bioactivity, reduce the occurrence of complications, and enable targeted therapy.

This review provides a detailed presentation of the biocompatibility and degradability of engineered 3D scaffolds with an additional focus on their porosity, mechanical performance, and potential significance in bone regeneration in osteonecrosis. Additionally, the findings of previous studies are generalized and explored to expound the development and advantages of 3D scaffold-mediated therapy (Scheme 1). We believe that this review article provides a comprehensive overview of 3D scaffolds for enhanced bone regeneration in osteonecrosis. Promotion of the theoretical basis and the state of the art of the clinical application of 3D scaffold-assisted bone regeneration in osteonecrosis is the expectation of this review.

2. Characteristics of engineered three-dimensional scaffolds for bone regeneration in osteonecrosis

The implantation of 3D scaffolds is an important strategy for enhancing bone tissue regeneration [43]. Natural and synthetic materials have been investigated for the manufacture of 3D scaffolds for enhancing bone regeneration in osteonecrosis. In addition, mixtures of several materials have been used to achieve a balance of the desired physical and chemical properties. Materials whose potential for bone regeneration in osteonecrosis has been studied include organic materials, such as poly(lactide-*co*-glycolide) (PLGA) [32,39,44–47], poly(D,L-lactic-*co*-glycolide acid)-*block*-methoxy poly(ethylene glycol) (PLGA−mPEG) [48], poly(ε-caprolactone) (PCL) [49], Cervi Cornus Colla (CCC) [50], poly(ethylene glycol) maleate citrate (PEGMC) [51], polylactide (PLA) [52], poly(methyl methacrylate) (PMMA) [53], peptide-based hydrogel [33], hyaluronic acid [54], collagen [55], demineralized bone matrix (DBM) [25], and xenogeneic antigen-extracted cancellous bone (XACB) [56], and inorganic materials, such as calcium phosphate (CP) [57], β-tricalcium calcium phosphate (TCP) [39,48,58], hydroxyapatite (HA) [46,59–62], ceramic [63,64], bioglass [65], and porous titanium (Ti) [66]. These biomaterials are processed into engineered scaffolds through a variety of technologies and exhibit excellent biocompatibility, biodegradability, porosity, and mechanical performance. These characteristics are vital for the successful application of 3D scaffolds to enhance bone regeneration in osteonecrosis (Table 1).

2.1. Biocompatibility and degradability

Biocompatibility, which is one of the primary requirements for cell

Table 1
Engineered 3D scaffolds for bone regeneration of osteonecrosis.

Matrix	Bioactive factor	Fabrication technology	Property	Reference
PLGA	BMSCs co-expressing BMP-6 and VEGF genes	–	Biocompatibility, enhanced angiogenesis and bone regeneration	[45]
PLGA/TCP	Mg	Low-temperature rapid prototyping technology	Biocompatibility, porosity was 81.3% ± 3.5%, pore size was 411.5 ± 26.9 μm, connectivity of pores was 100%, compressive strength was 3.7 ± 0.2 MPa, degradation time exceeded 20 weeks, enhanced angiogenesis and bone regeneration	[44]
PLGA/TCP	Icariin	Low-temperature 3D printing technology	Biocompatiblity, porosity was 76.4% ± 0.33%, pore size was 435.7 ± 28.6 μm, well interconnected macropore structure, compressive strength was > 2.0 MPa, degradation time exceeded 15 weeks, osteoinductivity	[39,102]
PLGA/CPC	BMP-2, VEGF	Solid/oil/water emulsion solvent evaporation method	Biocompatibility, porosity was 62.13% ± 4.28%, pore size was 219.3 ± 29.40 μm, compressive strength was 6.60 ± 1.02 MPa, enhanced angiogenesis and bone regeneration	[40]
PLGA/HA	Simvastatin	Water/oil/water emulsion method	Biocompatibility, simvastatin released over 14 days, enhanced angiogenesis and bone regeneration	[32]
PLGA/HA	BMP-2	Water/oil/water emulsion method	Biocompatiblity, BMP-2 released over 7 days (> 20 ng/mL/day), enhanced angiogenesis and bone regeneration	[46]
PLGA/HA/PBAE	–	Free radical polymerization, solution combustion process	Injectability, biocompatibility, porosity was 50%, pore size was 100 μm, yield strength was 6 MPa	[47]
PLGA – mPEG	VEGF, VECs	Sol – gel transition process method	Injectability, thermo-sensitivity, biocompatibility, VEGF released over 30 days, enhanced angiogenesis and bone regeneration	[50]
PCL/TCP	BMMCs	Layer-by-layer 3D printing technology	Biocompatibility, functionally graded porosity (19.3% ± 12.5% at the proximal segment, 4.4% ± 3.0% at the middle segment, and 10.4% ± 5.3% at the distal segment of the scaffold, respectively), biodegradability, enhanced angiogenesis and bone regeneration	[2,48]
PCL/CCC/deproteinized bone powder	–	Fused deposition modeling 3D printing technology	Biocompatibility, porosity was 72.86% ± 5.45%, pore size was 315.70 ± 41.52 nm, compressive strength was 6.27 ± 0.96 MPa, degradation time exceeded six weeks, enhanced bone regeneration	[49]
PLA	Adenoviral vectors carrying *til-1/Cbfa1* genes	–	Biocompatibility, enhanced bone regeneration	[52]
HA/gelatin	Li, EPO	Chemical precipitation method	Biocompatibility, porosity was 72.8% ± 4.6%, pore size was 200 – 300 μm, compressive strength was 3.5 MPa, degradation time exceeded 30 days, Li and EPO released over 30 days, enhanced angiogenesis and bone regeneration	[59]
HA/polyamide	BMMCs	–	Biocompatibility, enhanced bone regeneration	[61]
HA/type I collagen	Mg	Chemical cross-linking, freeze-drying, and self-assembly techniques	Biocompatibility, flexural properties, 3-layer biomimetic structure, enhanced cartilage and bone regeneration	[55]
HA/PEGMC/PEGDA	–	Sol – gel gelatin	Injectability, biocompatibility, pore size was 200 – 400 μm, compressive modulus was 205 ± 26 kPa, degradation time exceeded 22 weeks	[51]
Ceramic	–	Stereolithography technology	Biocompatibility, porosity was 45%, pore size was 600 – 800 μm, compressive strength was 23.54 MPa	[64]
CP	Sr, BMMCs	–	Biocompatibility, porosity was around 86%, enhanced angiogenesis and bone regeneration	[57]
TCP/DPI	–	Adsorption/freeze-drying strategy	Biocompatibility, BMSCs affinity, porosity was around 75% ± 10%, enhanced bone regeneration	[58]
Ti/gelatin	PRP	Laser sintering technology	Biocompatibility, porosity was approximately 91%, pore size was 100 – 250 μm, compressive strength was 6.27 ± 0.96 MPa, growth factors released over 21 days, enhanced bone regeneration	[66]
PPF/TiO_2	Ginsenoside Rg1, Sr	Sol – gel gelation, transesterification method	Biocompatibility, radiopacity, flexural strength was 41.5 ± 5.4 MPa, ginsenoside Rg1 released over 40 days, enhanced angiogenesis	[53]
Peptide-based hydrogel	BMP-2	Self-assemble technique	Injectability, biocompatibility, enhanced bone regeneration	[33]
Hyaluronic acid/Bisphosphonate/CaP	–	Chemical reaction method, gelation	Injectability, strong adhesion, self-healing, biocompatibility, enhanced angiogenesis and bone regeneration	[54]
DBM	Adenovirus-mediated expression of BMP-2 and bFGF in BMSCs	–	Biocompatibility, maintaining the organic matrix and growth factors, enhanced angiogenesis and bone regeneration	[25]
XACB	bFGF-transfected BMSCs	–	Biocompatiblity, enhanced angiogenesis and bone regeneration	[56]

DPIYALSWSGMA peptide (DPI), poly(propylene fumarate) (PPF).

adhesion, proliferation, and migration is also necessary to ensure that biomaterials do not cause harmful biological effects [43,67]. In the osteonecrotic microenvironment, the disruption of blood supply obstructs the excretion of metabolites. Therefore, unlike in normal bone defects, enhanced bone regeneration in osteonecrosis requires that the engineered 3D scaffolds possess stronger biocompatibility in order to avoid complications, such as immunological rejection.

Appropriate degradability is also an essential feature for an 3D scaffold. Degradability allows the materials to merge with the newly formed tissue and promotes the release of drugs loaded in the 3D scaffolds [68,69]. Osteonecrosis commonly occurs in joints, such as the hip joint. The anatomical structure of the joint is complex, and surgery is challenging and prolonged in duration. Therefore, removal of bone grafts causes considerable damage to the patient. After the implanted 3D scaffolds have achieved bone regeneration, their complete degradation without the formation of toxic by-products is the key to solve this problem. In addition, bone regeneration in osteonecrosis is often impeded, owing to impaired osteogenic capability [70,71]. This requires the 3D scaffolds to maintain structural stability while exhibiting controlled degradation in order to avoid incomplete bone regeneration due to inappropriate degradation.

In these respects,3D scaffolds manufactured using a combination of different materials have outstanding advantages. For example, although HA, a natural polysaccharide, has outstanding biocompatibility, its degradability is poor. The addition of lithium (Li) overcomes this limitation and enhances the toughness and osteoinductive ability of pure HA [60,72]. Based on this theory, Li and co-workers incorporated Li into the nano-hydroxyapatite (nHA) to construct Li-nHA engineered 3D scaffolds, which showed excellent biocompatibility and degradability [59].

In recent studies, researchers have produced an engineered 3D PLGA/TCP scaffold (Fig. 1A) [44,73]. This 3D scaffold, which was made of organic and inorganic materials, exhibited both excellent biocompatibility and biodegradability and exhibited improved mechanical performance. The 3D scaffold exhibited excellent adhesion and proliferation behaviors of bone marrow mesenchymal stem cells (BMSCs) on the 3D scaffold (Fig. 1B), and its degradation matched with the new bone ingrowth and remodeling (Fig. 1C).

2.2. Porosity

Ideal engineered 3D scaffolds should have a porous structure similar to that of healthy bone tissue, and the porosities of compact bone and cancellous bone in humans are 5%–10% and 50%–95%, respectively [74]. Pore structure allows cells to adhere to the 3D scaffolds and proliferate. In addition, appropriate pore size and interconnection between the pores also play critical roles in promoting bone tissue growth into the 3D scaffolds [75]. Numerous studies indicate that the optimal pore size ranges from 100 to 500 μm [76–78]. The pores and interconnected channels in the 3D scaffolds promote nutrient and oxygen transport for penetration of cells and boost angiogenesis [79–81]. In osteonecrosis, the obstruction of blood supply, especially microcirculation, is one of the main reasons for the disruption of bone regeneration [40]. Therefore, engineered 3D scaffolds should possess excellent porosity and interconnected porous structures in order to achieve rapid angiogenesis and facilitate the delivery of high levels of oxygen to the necrotic region, thus enabling the differentiation of BMSCs into osteoblasts.

Among the various processing technologies, 3D printing technology has clear advantages in producing the scaffolds with appropriate porosity, controllable pore size, and interconnected channels, owing to its ability to form complex 3D geometries [43,82,83]. Lai *et al.* [39] engineered an advanced porous 3D PLGA/TCP/Icariin (PTI) scaffold using a low-temperature 3D printing technology to accelerate the regeneration of the osteonecrotic area in steroid-associated osteonecrosis (SAON). The 3D scaffold had a porosity of approximately 79.5%, a pore size of approximately 435.7 μm, and large interconnected pore structures, which made its structure very similar to that of healthy cancellous bone. Consistent with these findings, studies *in vivo* also support the therapeutic effect of the porous 3D scaffolds.

Functionally graded scaffolds (FGS) with differential porosity were designed and manufactured by 3D printing with PCL and TCP as the matrix [2]. The porosities of the manufactured 3D scaffolds were approximately 16.8% for the proximal, 59.5% for the middle, and 16.4% for the distal segments, respectively (Fig. 2A − C). Their structure was very similar to the pore structure of the subchondral bone of the femoral head, the cancellous bone of the femoral head, and the cortical bone of the lateral wall of the greater trochanter, respectively. *In vivo*, visible mineralization within the 3D scaffolds elicited excellent pore connectivity and bone repair ability (Fig. 2D − E).

2.3. Mechanical performance

The skeleton plays a vital role in providing structural support, organ protection, mobility, and withstanding functional load bearing for the body [84,85]. Excessive porosity and pore size impair the structural integrity of the scaffold, resulting in reduced mechanical performance [78]. Therefore, the mechanical performance of the 3D scaffolds should not be overlooked in the pursuit of high levels of porosity. 3D scaffolds should meet the local mechanical requirements in order to achieve a balance between porosity and mechanical performance. Osteonecrosis usually involves large joints, which are the weight-bearing parts of the body [86–88]. Therefore, during bone regeneration in the treatment of osteonecrosis, insufficient mechanical strength in the necrotic area renders the new tissue vulnerable to damage by external forces, leading to failure of repair [64]. Biomechanical support of the local area should be maintained throughout the management period until the neighboring tissue is fully regenerated and able to undertake its structural role [89].

Owing to advancements in biological and material sciences, increasing evidence for the importance of mechanical performance in osteonecrosis is reported. In addition to its excellent tissue affinity and biodegradability, the inherent microporous structure and mechanical performance of calcium phosphate cement (CPC) warrant attention [40]. Zhang *et al.* [40] used CPC to strengthen bone regeneration in osteonecrosis. PLGA microsphere loaded with growth factor was prepared and then combined with CPC to form a 3D composite scaffold. These compositions provided superior compression strength while ensuring porosity and interconnectivity of pores. Biomechanical studies have shown that the compressive strength of 3D scaffolds (6.60 MPa) was similar to that of healthy cancellous bone and enabled the immediate restoration of load function.

Similarly, mixing synthetic polymers with inorganic materials to fabricate composite 3D scaffolds is a common strategy to enhance biomechanical performance. Gyawali and co-workers designed an injectable 3D scaffold composite comprising PEGMC, poly(ethylene glycol) diacrylate (PEGDA), and HA [51]. The composite 3D scaffold had excellent elastic properties and mechanical strength, and similar compression strength compared with the acellular cancellous bone of a porcine model.

DBM, which is derived from bone, is inexpensive and readily available. It comprises an organic matrix and a small quantity of growth factor, which makes it osteoconductive and confers excellent mechanical performance [25,90]. Peng *et al.* [25] used DBM combined with adenovirus-mediated bone morphogenetic protein-2 (BMP-2) and basic fibroblast growth factor (bFGF)-transfected BMSCs to regenerate bone tissue in a canine model of ONFH. After 12 weeks, testing of the compressive strength and bending strength of tissue specimens revealed that the group that received DBM and BMP-2 − bFGF-transfected stem cells exhibited the most significant mechanical performance (Fig. 3A and B). The bone morphology of the composite materials group was superior to that of the control group at 12 weeks after surgery (Fig. 3C).

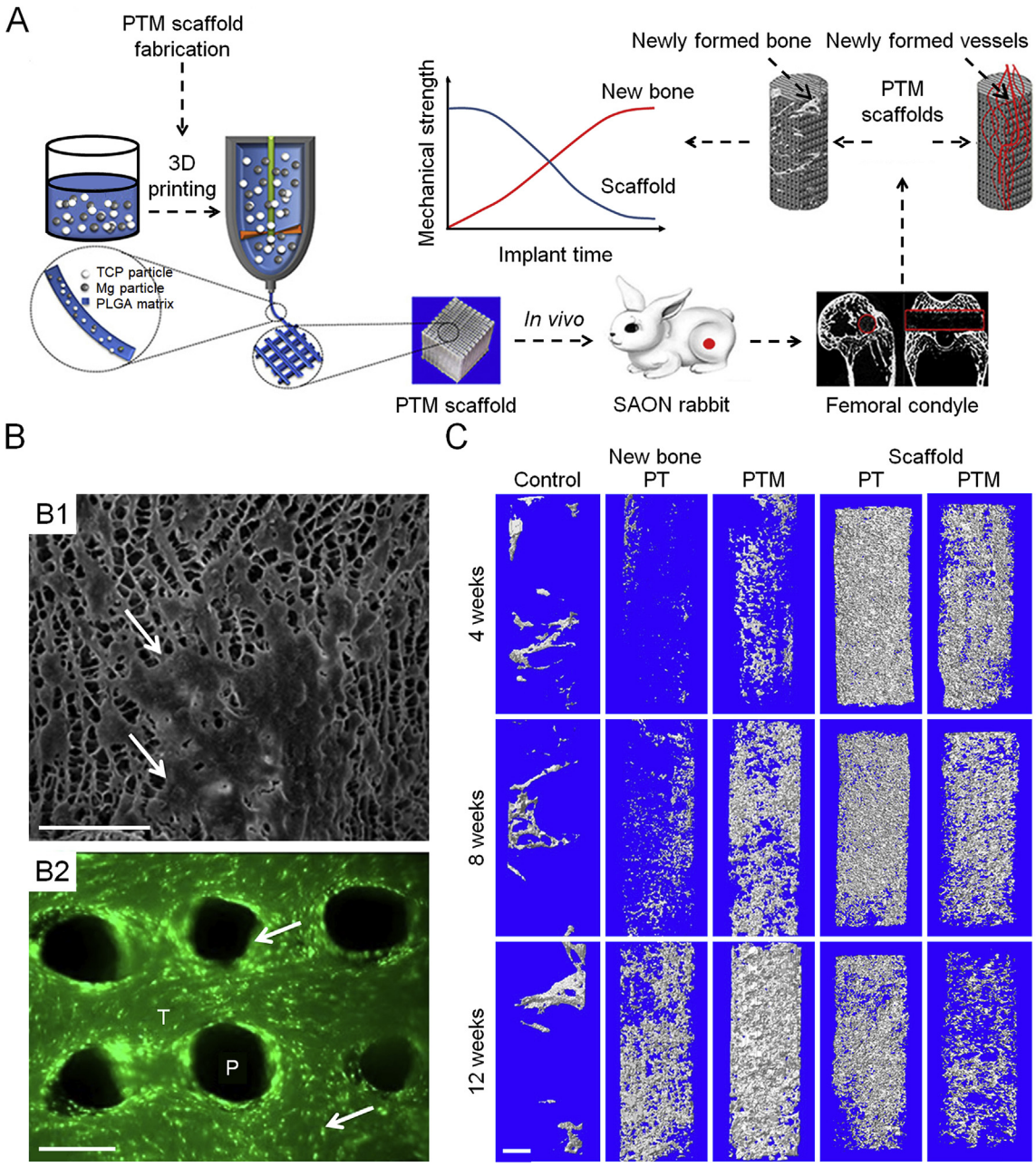

Fig. 1. Manufacture of 3D PLGA/TCP scaffold with excellent biocompatibility and biodegradability for bone regeneration in osteonecrosis [44,73]. (A) Porous PLGA/TCP (PT) and PLGA/TCP/Mg (PTM) scaffolds produced by 3D printing technology and their *in vivo* test [44]. (B) SEM (B1) and fluorescent microscope (B2) observation for attachment and morphology of BMSCs (arrows) seeded on scaffolds after 24 h and 15 days, respectively. T denotes trabeculae of scaffolds, and P denotes pores of scaffolds. Scale bar, B1 = 50 μm, B2 = 500 μm [73]. (C) Micro-CT images of the new bone formation and the residue of PT and PTM scaffolds in bone tunnel at each time point after surgery. Control group represents surgery without scaffold implantation. Scale bar = 1 mm [44]. Reproduced with permission [44]. Copyright 2019, Elsevier Ltd. Reproduced with permission [73]. Copyright 2012, John Wiley & Sons, Ltd.

In addition to the properties mentioned above, 3D scaffolds should possess good hydrophilicity, surface roughness, specific surface area, and osteoconductivity, and additionally be injectable and easy to prepare [54,91,92]. In conclusion, on the premise of ensuring biocompatibility and degradability of 3D scaffolds, bone regeneration in osteonecrosis requires 3D scaffolds to replicate highly porous bone structures and possess the ability to provide adequate mechanical support for local tissue, which is a major challenge for researchers in this field. The combination of natural materials and synthetic polymer materials offers an outstanding solution in this context.

3. Engineered three-dimensional scaffold-mediated bone regeneration in osteonecrosis

Strategies to enhance bone regeneration should be implemented as early as possible to avoid severe consequences like joint collapse. The combination of core decompression (CD) and bone grafting is commonly used for clinical treatment of osteonecrosis. Owing to their characteristics, *e.g.,* biocompatibility, biodegradability, porosity, and mechanical performance, engineered 3D scaffolds have clear advantages as bone graft substitute materials, thus allowing the limitations of autografts and allografts, such as source limitations, immune rejection, infection, and difficulty in shaping, to be overcome [34,35].

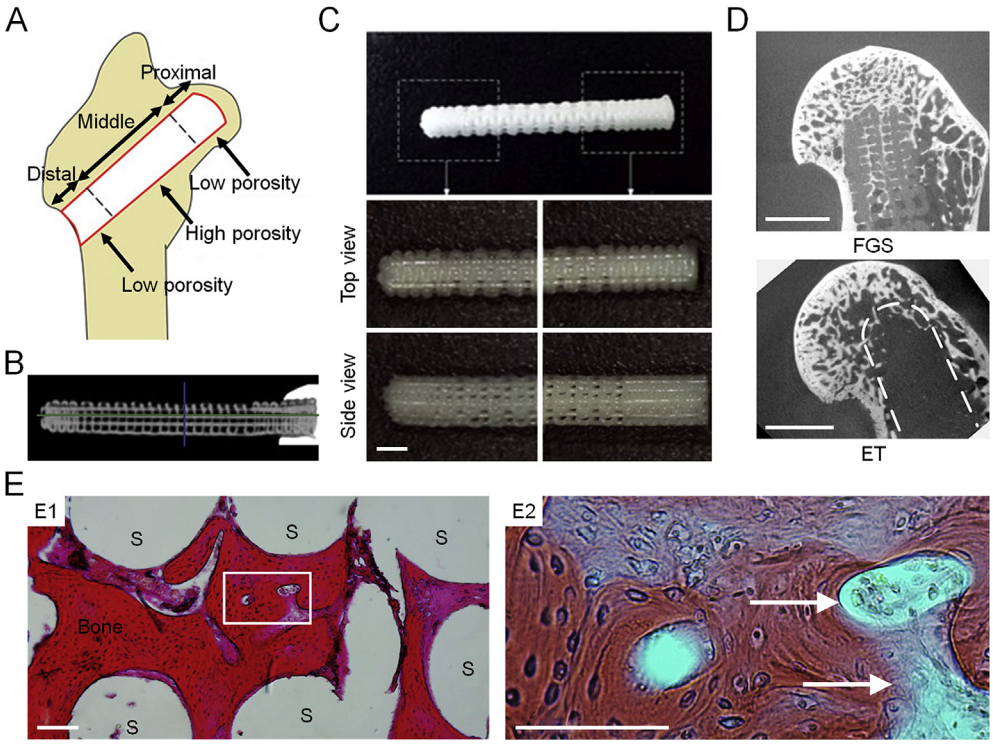

Fig. 2. 3D scaffolds with different porosities in different parts for enhanced bone regeneration in osteonecrosis [2]. (A) Graphic image shows how the three segments of FGS with different porosity were distributed in the femoral head. (B) Micro-CT showed that the scaffolds had three different porosity segments and excellent pore connectivity. (C) An external view of FGS with magnified view. Scale bar = 2 mm. (D) Micro-CT image of FGS-implanted group (FGS) and empty-tunnel group (ET) after drilling of rabbit femoral head. Drilled tunnel was indicated by a dashed line. Scale bar = 5 mm. (E1) Representative hematoxylin and eosin (H&E) staining observed new bone formation. S refers to scaffolds. Scale bar = 100 μm. (E2) Magnified image of the region depicted by a rectangle in E1. Blood vessels coexisting with osteon-like structures were indicated by arrows. Scale bar = 100 μm. Reproduced with permission [2]. Copyright 2017, John Wiley & Sons, Ltd.

However, materials without osteogenic factors, bioactive molecules, or seeded cells have a limited therapeutic effect [93]. For this problem, various bioactive factors were used to functionalize 3D scaffolds to improve the osteoinductivity in osteonecrosis. A variety of functionalized 3D scaffolds were developed, and their efficacies for bone regeneration were demonstrated in various animal models (Table 2) [25,32,39,40,46,48–50,54,56,57,59,63,66,94–102].

3.1. Combination of three-dimensional scaffolds and cells

3.1.1. Three-dimensional scaffolds and stem cells

In the past years, a combination of 3D scaffolds and cells represents an effective management strategy for bone regeneration in osteonecrosis. Mesenchymal stem cells are characterized by their ability to differentiate into several cell lineages (*e.g.*, osteocytes, osteoblasts, and endothelial cells) and possess the homing ability to injury sites [95,103,104]. BMSCs are easy to culture and amplify *in vitro* and accelerate bone healing through differentiation into osteoblasts [105,106]. Therefore, these cells are of significant interest in the field of bone regeneration in osteonecrosis. Moreover, studies have shown that BMSCs are decreased in number and activity in patients with osteonecrosis [107]. These findings indicate that stem cells play a vital role in the repair of necrotic areas.

3D scaffolds effectively target BMSCs to necrotic areas and provide mechanical support for them, while stem cell seeding functionalizes the 3D scaffolds. Various inorganic materials, such as biphasic calcium phosphate (BCP) and HA, may be used for this strategy. Peng *et al.* [108] constructed 3D BCP ceramic scaffolds with seeded BMSCs. *In vitro* studies showed that the 3D scaffolds demonstrated good biocompatibility and mechanical performance, which were beneficial for seeding cells. Increased new bone formation at bone defect sites in a canine model was observed after implantation of functionalized 3D scaffolds. Therefore, this may represent a promising strategy for enhancing bone regeneration in osteonecrosis. In addition, modification of the 3D scaffolds using peptides with affinity to BMSCs enhanced the adhesion of functionalized 3D inorganic scaffolds to BMSCs, representing an additional improved method to enhance bone regeneration in osteonecrosis [58].

Some metal 3D scaffolds are also suitable for loading BMSCs. Porous tantalum (Ta) has excellent porosity, biocompatibility, and mechanical performance, and is conducive to the loading of stem cells following appropriate surface modification [38,109,110]. Recently, Liu and coworkers established a functionalized 3D scaffold based on porous Ta, covered with the Bio-Gide® collagen membrane, and seeded with BMSCs [38]. The cells exhibited excellent morphology and adhesion, and the foot processes extending out from the cell bodies were connected and oriented in various directions (Fig. 4A－B). Compared with that of the other groups, the new cartilage in the group of 3D scaffolds loaded with BMSCs was thicker and showed superior morphology *in vivo* (Fig. 4C).

In addition, appropriate pretreatment is beneficial to enhance the therapeutic effects of BMSCs. Hypoxic pretreatment induces a compensatory response in BMSCs through the activation of endogenous mechanisms, increases viability, and reduces the apoptosis of cells during implantation. Furthermore, hypoxia pretreatment has the effect of enhancing the expression of angiogenic growth factors [95,111]. In combination with the 3D scaffolds, this represents an excellent strategy. Fan *et al.* [95] functionalized absorbable collagen sponge with hypoxia-pretreated BMSCs and achieved effective bone regeneration and angiogenesis. In another study, Li *et al.* [60] designed and fabricated 3D Li-doped HA scaffolds, which were demonstrated to exhibit excellent biological properties. Functionalized 3D scaffolds seeded with hypoxia-pretreated BMSCs showed commendable potential for osteogenesis and angiogenesis.

Inducing selective differentiation of stem cells using growth factors before stem cells combining with scaffolds is an additional promising option. Seeding bFGF-transfected BMSCs onto tissue-engineered bone effectively increased the density of new blood vessels, regenerated osseous tissue, and resolved the problem of the short half-life of bFGF [56]. Peng *et al.* [25] synthesized adenovirus-mediated BMP-2 and bFGF modified BMSCs to functionalize DBM. The application of functionalized 3D scaffolds increased the area of new bone and density of neovascularization, confirming that this strategy was highly effective.

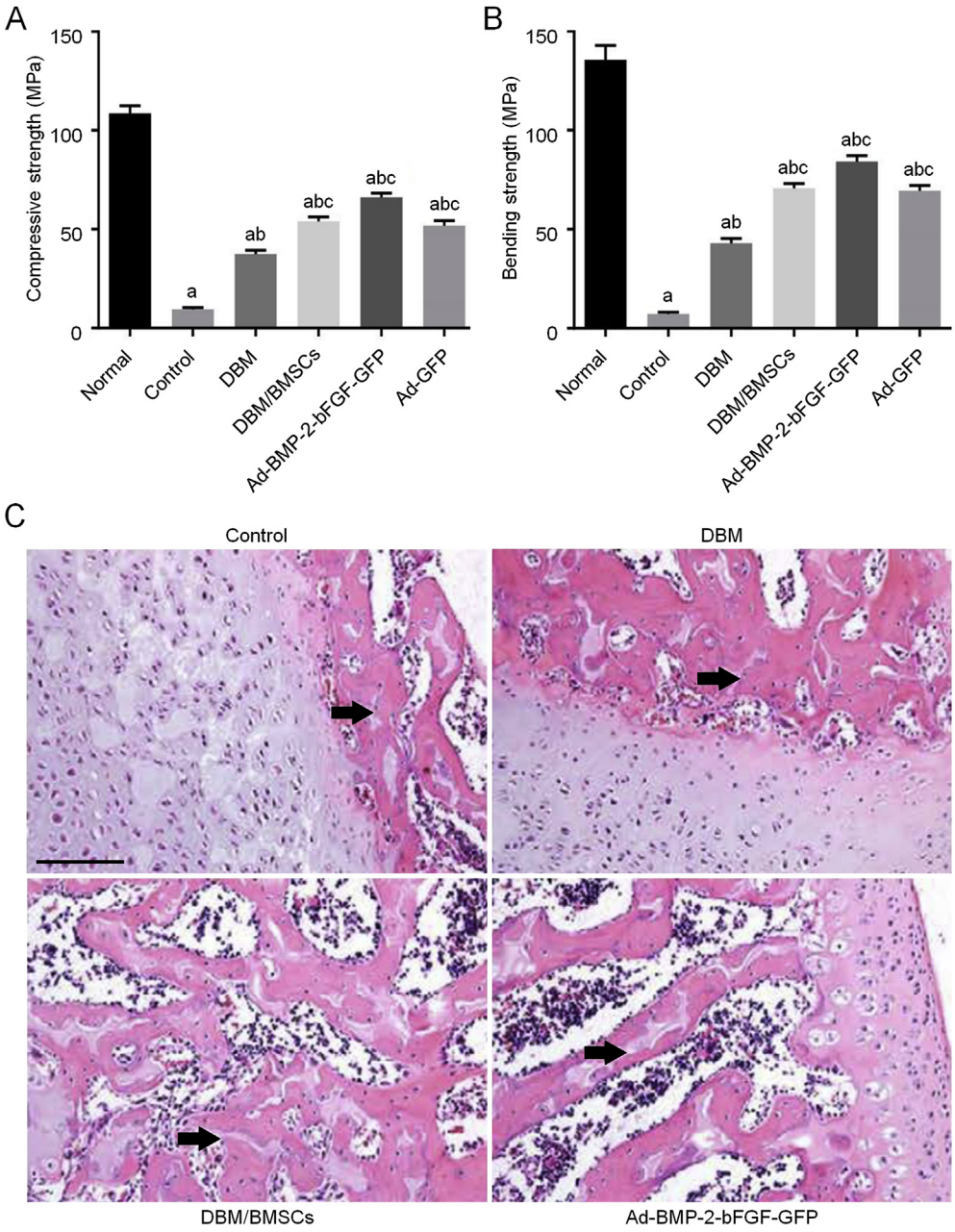

Fig. 3. Role of 3D scaffolds with different mechanical performances in promoting bone regeneration in osteonecrosis [25]. (A,B) The compressive (A) and bending strength (B) testing results at 12 weeks after surgery. Normal means normal canine bone without osteonecrosis, Control means necrotic bone without therapy, DBM means treated necrotic bone by DBM, DBM/BMSCs means treated necrotic bone by DBM and BMSCs, Ad-BMP-2-bFGF-GFP means treated necrotic bone by DBM and BMSCs transfected with adenovirus vector plasmid containing BMP-2 and bFGF, and Ad-GFP means treated necrotic bone by DBM and BMSCs transfected with adenovirus vector plasmid. All $P < 0.05$ by Student-Newman-Keuls (SNK) method. (C) H&E staining images of the canine model at 12 weeks after surgery. Black arrow indicates trabecular bone. Scale bar = 100 μm.

3.1.2. Three-dimensional scaffolds and bone marrow-derived mononuclear cells

Bone marrow-derived mononuclear cells (BMMCs) are also commonly loaded onto 3D scaffolds to enhance bone regeneration in osteonecrosis. Many studies have confirmed that BMMCs have stimulatory effects on both vascularization and osteogenesis, with distinct advantages in enhancing bone regeneration in osteonecrosis [112,113]. A decade ago, Yamasaki *et al.* [114] used porous HA scaffolds combined with BMMCs for clinical management. The functionalized 3D scaffold effectively promoted bone regeneration in osteonecrosis. Subsequently, Kang *et al.* [57] constructed 3D scaffolds of strontium (Sr)-doped TCP seeded with BMMCs and analyzed their therapeutic effects. The functionalized 3D scaffolds had excellent porosity, conducive to the proliferation of BMMCs. Furthermore, penetration of newly formed bone through the functionalized 3D scaffolds was observed by studies. These findings suggest that 3D scaffolds seeded with BMMCs have a positive effect on bone regeneration in osteonecrosis.

Recently, Maruyama *et al.* [48] manufactured and utilized 3D PCL/β-TCP matrix scaffolds loaded with BMMCs for enhanced bone regeneration in SAON. This functionalized 3D scaffold exhibited an excellent porosity and mechanical performance, and had excellent bone repair capability. In particular, compared with cell therapy alone, functionalized 3D scaffolds had a higher percentage of bone ingrowth and reduced numbers of empty lacunae (Fig. 5), thereby demonstrating decreased necrotic area and promoting healing. This suggested that cell therapy achieved better performance mediated by the 3D scaffolds than when used alone.

3.1.3. Three-dimensional scaffolds and stromal vascular fraction cells

Stromal vascular fraction cells (SVFs) are derived from human adipose tissue, including mesenchymal progenitors, endothelial cells, and so forth [115,116]. SVFs are useful in accelerating the ingrowth of tissue and ensuring uniformity of the structure of bone tissue. Moreover, SVFs support the regeneration of vascular structure, especially the capillary network [117]. Engineered 3D scaffolds facilitate seeding of SVFs and construct a 3D culture system for SVFs, referred to as

Table 2
Animal model established in engineered 3D scaffolds for enhanced bone regeneration in osteonecrosis.

Animal	Induced protocol	Induced approach	Operating times	Remark	Reference
Rabbit	10.0 μg/(kg BW) LPS	Intravenous injection	Once	LPS and MPS were administered 24 h apart	[39,59,94,95]
	20.0 mg/(kg BW)/day MPS	Intramuscular injection	Thrice		
Rabbit	20.0 mg/(kg BW)/day MLPS	Intramuscular injection	Once	Model was constructed after 4 weeks	[48,57,96]
Rabbit	10.0 mL/(kg BW) HS	Intravenous injection	Once	The interval between 10.0 mL/(kg BW) HS and 5.0 mL/(kg BW) HS and PSL was two weeks, and PSL was injected twice a week	[40,97]
	5.0 mL/(kg BW)/day HS	Intravenous injection	Twice	(7.5 mg/(kg BW))	
	15.0 mg/(kg BW)/week PSL	Intraperitoneal injection	Twice		
Rabbit	10.0 μg/(kg BW)/day endotoxin	Intravenous injection	Twice	Endotoxin and MPS were administered 24 h apart	[56]
	40.0 mg/(kg BW)/day MPS	Intramuscular injection	Thrice		
Rabbit	Anhydrous alcohol	Bone injection	–	Model was constructed after 4 weeks	[50]
Rabbit	Frozen using liquid nitrogen	Surgery	Once	The location was femoral head	[54,66]
Rabbit	Microwave inactivation	–	10 min	–	[63]
Rabbit	Cut off the femoral neck	Surgery	Once		[98]
Rat	100.0 μg/(kg BW) LPS	Intravenous injection	Once	LPS and MPS were administered 24 h apart	[99]
	40.0 mg/(kg BW)/day MPS	Intramuscular injection	Thrice		
Rat	10.0 μg/(kg BW) LPS	Intravenous injection	Once	LPS and MPS were administered 24 h apart	[100]
	20.0 mg/(kg BW)/day MPS	Intramuscular injection	Thrice		
Rat	20.0 mg/(kg BW)/day MPS	Intramuscular injection	Nine times	The injection was on the first three days of every week for three weeks	[101]
Rat	0.14 g/(kg BW)/day retinoic acid	Oral gavage	56 times	–	[49]
Mouse	Frozen using liquid nitrogen	Surgery	Once	The location was the middle shaft of the tibia	[32]
Mouse	Stripped the whole periosteum	Surgery	Once	The location was the middle shaft of the tibia	[46]
	Frozen using liquid nitrogen	Surgery	Once		
Dog	Drill holes in the weight-bearing area	Surgery	Once	The full-thickness defect was located at the femoral head	[25]
Emu	8.0 μg/(kg BW)/4 days LPS	Intravenous injection	Twice	LPS and MPS were administered 4 days apart	[102]
	10.0 mg/(kg BW)/2 days MPS	Intramuscular injection	Thrice		

Horse serum (HS), lipopolysaccharide (LPS), methylprednisolone (MPS), methylprednisolone acetate (MLPS), prednisolone acetate (PSL).

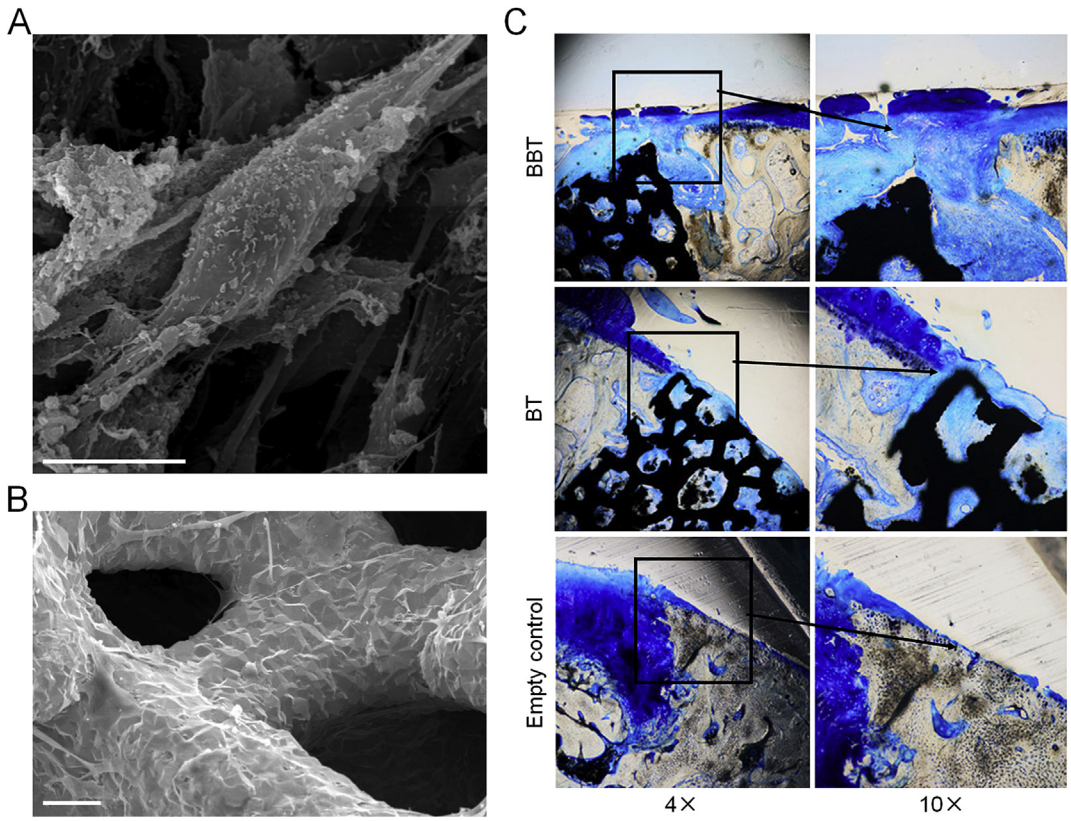

Fig. 4. Combination of 3D scaffold with BMSCs for enhanced bone regeneration in osteonecrosis [38]. (A) SEM image after 21 days of co-culture of BMSCs with Bio-Gide® collagen membrane. Scale bar = 10 μm. (B) Image of BMSCs co-cultured with porous Ta scaffold observed by SEM after 21 days. Scale bar = 10 μm. (C) Toluidine blue staining at 12 weeks after surgery. Empty control refers to the full-thickness articular defect of femoral head without implantation, BT refers to the defect filled with 3D scaffolds composed of Bio-Gide® collagen and porous Ta, BBT refers to the defect filled with 3D scaffolds composed of BMSCs, Bio-Gide® collagen, and porous Ta, the black square was the enlarged area. Reproduced with permission [38]. Copyright 2019, Elsevier Ltd.

osteogenic-vasculogenic constructs [117,118]. This advanced synthesized bone graft has outstanding intrinsic vascularization and rapid engraftment ability. On this basis, it was shown that SVF-based functionalized 3D scaffolds induced the regeneration of bone necrotic regions [119].

Cell therapy is a promising therapeutic concept. However, it is difficult to achieve the ideal concentration of cells at the location of the lesion, owing to the pathological changes that occur during osteonecrosis. The mediation of 3D scaffolds allows the cells used for treatment to reach the deepest part of necrotic area, thus achieving the full play to the therapeutic effect for a sustained release manner. Further, cell seeding enhances the therapeutic potential of 3D scaffold. Therefore,

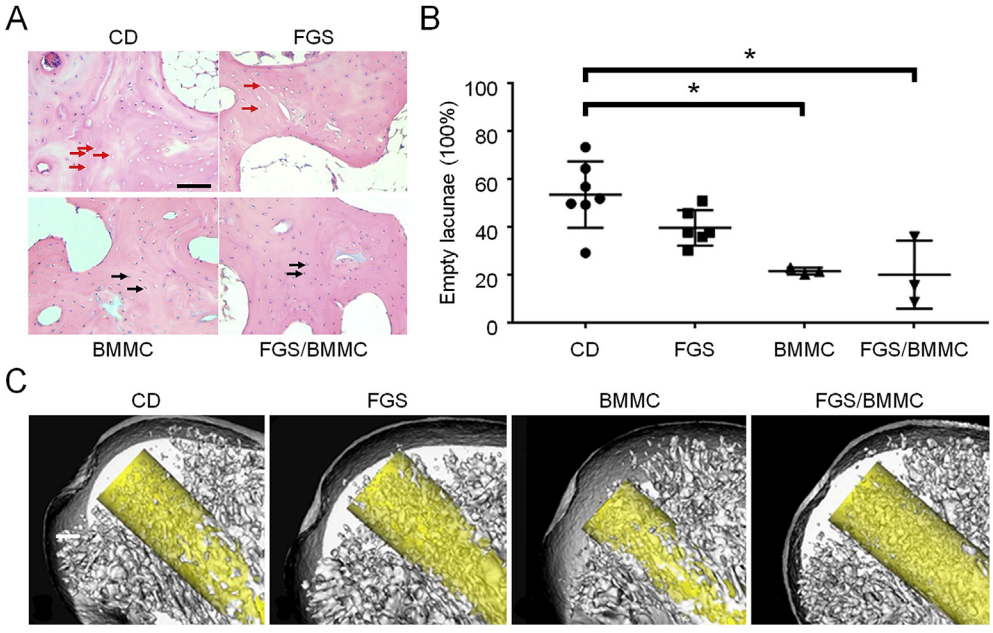

Fig. 5. Engineered 3D FGS combined with BMMCs decreased necrotic area and enhanced bone regeneration in osteonecrosis [48]. (A) H&E staining in each group. CD refers to core decompression only, FGS refers to CD and FGS filled in, BMMC refers to CD and BMMCs injected in, FGS/BMMC refers to CD, and functionalized FGS combined with BMMCs filled in. The red arrow denotes empty lacunae, and the black arrow denotes normal osteocyte. Scale bar = 200 μm. (B) Percentage of the empty lacunae in each group. Asterisk * indicates $P < 0.05$ by Dunn post-hoc test. (C) Micro-CT reconstructed images of the drill channel in femoral heads. Reproduced with permission [48]. Copyright 2018, 2018 Elsevier Ltd.

functionalizing 3D scaffolds by combining with cells is of great therapeutic significance in osteonecrosis.

3.2. Combination of three-dimensional scaffolds with growth factors

Growth factors have been widely used in bone regeneration of osteonecrosis, owing to their capacity to accelerate the differentiation of stem cells into osteoblasts and stimulate the generation of blood vessels [120,121]. However, problems, such as loss of biological activity, short of half-life *in vivo*, relatively short storage period, and heterotopic ossification related to the applications of growth factors, remain to be solved [33,56,122]. In this context, the emergence of 3D scaffolds has provided excellent prospects. As a vehicle, 3D scaffolds effectively preserve the bioactivity of growth factors, stabilize the latter in the targeted region, and ensure sustained release. In addition to binding to 3D scaffolds by transfection of stem cells, as mentioned above, the direct binding of growth factors to form functionalized 3D scaffolds shows promising therapeutic efficacy.

3.2.1. Three-dimensional scaffolds and bone morphogenetic proteins

-BMPs are members of the transforming growth factor-β (TGF-β) superfamily and play a key role in promoting bone formation [123]. Among the various known endogenous growth factors, BMPs are one of the most effective osteoinductive proteins. BMPs stimulate osteogenic differentiation and enhance the activity of osteoblasts [124,125]. In addition, BMPs are effective stimulators of new vascularization [126]. However, as a protein substance, loss of activity and structural instability are the main problems that limit the application of BMPs, and a medium, *e.g.*, 3D scaffold, is therefore required. Therefore, the combination of BMPs and 3D scaffolds has obvious potential for accelerating bone regeneration in osteonecrosis.

Injectable hydrogels, a popular carrier for growth factors, are rapidly converted from sol to gel, and then degraded to release the loaded growth factors [127]. Peptide-based hydrogels contained β-sheets, which optimized all aspects of the performance of the hydrogel and promoted new bone formation, as shown by Phipps and co-workers [33], who used peptide-based hydrogels as a vehicle to deliver of BMP-2 efficiently. When mixed with a radiocontrast agent, functionalized hydrogel effectively prevented the backflow of BMP-2 in cadaver pig femoral heads, which was necessary for reducing heterotopic ossification after treatment (Fig. 6).

An alternative strategy involves sealing growth factors within the structure of microsphere, which maintains the activity and sustained release of the factors. Wang *et al.* [46] encapsulated BMP-2 in the PLGA-nHA microsphere and found that the device released sufficient therapeutic concentrations of BMP-2. The biological activity of BMP-2 was well maintained, and prominent bone creeping in the necrotic region was observed, which effectively facilitated bone regeneration in osteonecrosis.

3.2.2. Three-dimensional scaffolds and vascular endothelial growth factor

Vascular endothelial growth factor (VEGF) is regarded as a critical regulator of physiological angiogenesis during bone growth and reconstruction [128]. VEGF promotes the growth of vascular endothelial cells (VECs), stimulates revascularization of the necrotic site, and promotes capillary formation, while also inducing osteoblast adhesion and proliferation, and promoting new bone formation [40,129]. Therefore, the crucial role of VEGF in bone regeneration in osteonecrosis is self-evident. The engineered 3D scaffold-mediated approach is conducive to achieving the full therapeutic potential of VEGF in this context.

Block copolymers have attractive hydrophilicity, biodegradability, high loading rate for growth factors, and sustained release ability. Chen *et al.* [50] studied the activity of 3D scaffold formed by PLGA-*b*-mPEG, and then loaded VEGF onto this scaffold. The release of VEGF and the proliferation of endothelial cells were found to be excellent. The density and diameter of new blood vessels increased together with the formation of new bone, indicating that the scaffolds loaded with VEGF were conducive to bone regeneration in osteonecrosis.

Many studies have found that the combined use of BMP-2 and VEGF has a synergistic effect on tissue regeneration that is superior to that achieved when either is used alone [129,130]. Zhang *et al.* [40] achieved the co-loading of BMP-2 and VEGF in the PLGA microspheres and formed a functionalized 3D scaffold together with CPC. This 3D scaffold itself had ideal biocompatibility and a porous connection structure. When co-cultured with the functionalized 3D scaffold, cells presented remarkable osteogenic and angiogenic abilities (Fig. 7A and B). These results proved that dual-factor-loaded functionalized 3D scaffolds accelerated bone regeneration better than when one growth factor was used *in vivo* and additionally delayed the development of osteonecrosis (Fig. 7C and D).

3.2.3. Three-dimensional scaffolds and platelet-rich plasma

Platelet-rich plasma (PRP) is of interest because it contains many different autologous growth factors, such as VEGF, TGF, and epithelial growth factor [131]. Its advantages, when used in combination with 3D scaffolds, are mainly reflected in the effective multi-functional treatment ability. A combination of the advantages of various substances to achieve the optimal therapeutic strategy represents a promising research direction. For example, 3D scaffolds provide local mechanical support, while biomaterial coatings on their surface promote proliferation and adhesion of cells. Finally, PRP is introduced to functionalize the 3D scaffolds. Using this strategy, Zhu *et al.* [66] created a multi-functionalized 3D Ti/gelatin/PRP scaffold with the capacity to release growth factors stably. The functionalized 3D scaffolds exhibited excellent biosafety and elicited accelerated bone growth. These effects were also demonstrated in an animal model. In another study, TCP/PRP 3D scaffold was designed and manufactured by Zhang *et al.* [98] The area of new bone had significantly increased in the group of functionalized 3D scaffold. These studies collectively indicate that the 3D scaffold is an effective carrier of PRP for enhanced bone regeneration.

3.2.4. Three-dimensional scaffolds and erythropoietin

Erythropoietin (EPO) is a pleiotropic cytokine that stimulates the generation of blood vessels through various signaling pathways, enhances the performance of VEGF, and even accelerates the differentiation of BMSCs into osteoblasts [132–134]. The researchers used Li-doped nHA as a matrix to produce functionalized 3D scaffold through the attachment of gelatin microsphere and EPO [59]. In this functionalized 3D scaffold, which had excellent porosity and mechanical performance, cell culture showed that ALP expression was upregulated, calcium deposition was improved, and angiogenesis was enhanced. This group of functionalized 3D scaffold achieved the superior new bone formation and neovascularization in the implantation channel defect of the animal model than other groups. Therefore, this functionalized 3D scaffold was extremely useful for promoting bone regeneration in osteonecrosis.

Many therapies are aimed at promoting bone regeneration. In addition, the lack of functional vascular ingrowth in the tissue-engineered materials has been identified as the primary culprit for regenerative failure [135]. Adequate angiogenesis is necessary for the long-term survival of osteoblasts in 3D scaffolds [136]. Growth factors that are helpful for osteogenesis and angiogenesis offer a natural advantage in this context. Engineered 3D scaffolds are powerfully effective in transporting growth factors to the target site and maintaining their activity. Additionally, this strategy effectively avoids complications caused by the flow of growth factors to off-target sites.

3.3. Combination of three-dimensional scaffolds with small-molecule drugs

Small-molecule drugs play a critical role in the treatment of many diseases and are a popular therapeutic option in clinical settings. Small-molecule drugs have a molecular weight of less than 1000 Da, and

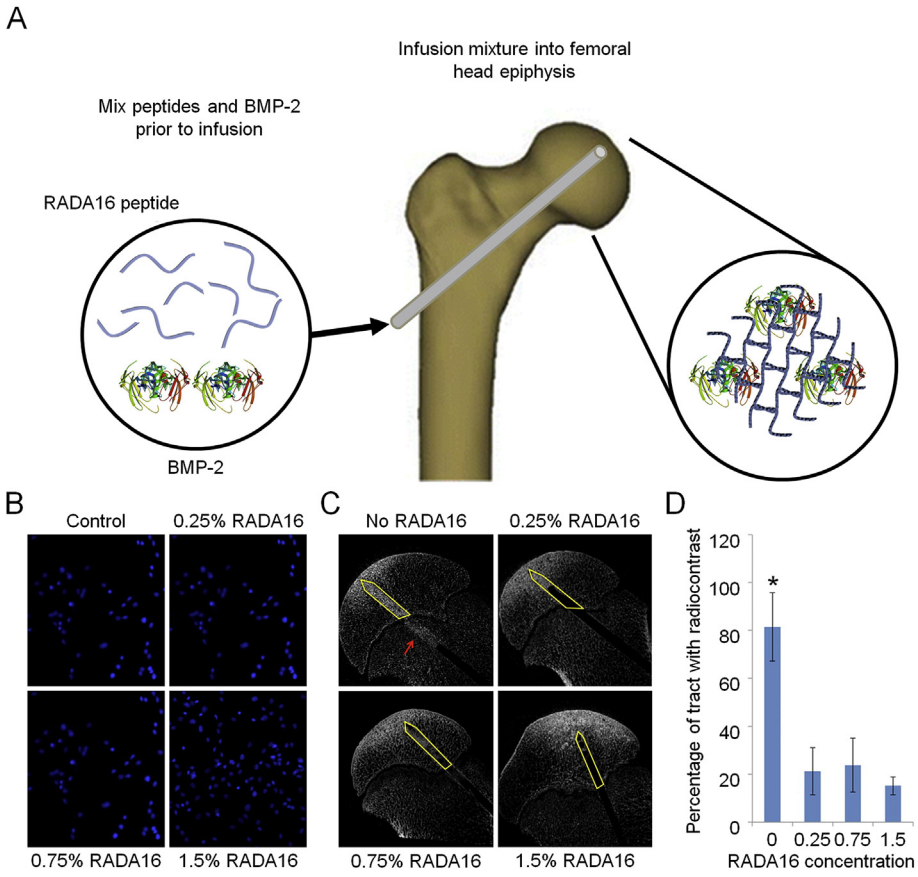

Fig. 6. Peptide-based hydrogel loaded with BMP-2 prevented ectopic ossification during management [33]. (A) The model was drilled and injected with functionalized hydrogel (B) Confocal microscopy images (20× magnification) showed the BMSC nuclei after 7 days of being cultured with tissue culture plastic (Control) or different concentrations of RADA16 (0.25%, 0.75%, and 1.5%) *in vitro*. (C) The micro-CT images showed the amount of backflow of the radiocontrast solution down the tunnel after being combined with the peptide-based hydrogel (RADA16) at different concentrations. The yellow outline indicates the tunnel inside the femoral head epiphysis, and the red arrow indicates the backflow of radioactive contrast outside the femoral head epiphysis. (D) Percentage of backflow of different concentrations of RADA16 in the tunnel. Asterisk * indicates the greater backflow compared with other test groups, $P < 0.05$ by Tukey's post-hoc test. Reproduced with permission [33]. Copyright 2016, American Chemical Society.

therefore rarely cause adverse immune reactions. Additionally, unlike growth factors, small-molecule drugs are often low-cost and stable, and do not necessarily require structural integrity [137,138]. Numerous small-molecule drugs have been developed to promote bone regeneration in osteonecrosis, for instance, anticoagulants, vasodilators, statins, vitamin D, scavenger of free radicals, and Chinese herb extracts, such as icariin, salidroside, and ginsenoside Rg1, have attracted extensive attention, owing to their effects against various adverse factors that hamper bone regeneration and cause bone destruction in osteonecrosis. However, the decline in biological activity, damage to other organs, and burst release are significant challenges that limit the clinical application of these therapies [31,32,139]. Engineered 3D scaffolds are increasingly recognized to have unparalleled advantages as drug carriers and represent effective alternatives [102,140].

3.3.1. Three-dimensional scaffolds and Chinese herb extracts

The advantages of Chinese herbs are recognized globally. In particular, extracts of the active components have attracted considerable attention. The Chinese herb epimedium has “kidney-tonifying and bone-strengthening” effects [141]. Icariin, an effective active extract of epimedium, promotes the activity and mineralization of osteoblasts, controls adipogenic differentiation of BMSCs, and promotes capillary tube formation [102,142–144]. Therefore, icariin meets the diverse requirements of bone regeneration in osteonecrosis.

Qin and his research team have made significant progress in the treatment of bone destruction in osteonecrosis using icariin-functionalized 3D scaffolds [39,102]. Recently, these authors developed a PTI-functionalized 3D scaffold based on PLGA, TCP, and icariin (Fig. 8A) [39]. Of particular note, because of the strengthened crosslinking enabled by hydrogen bonding between the polymer and icariin, the biodegradation and compressive strength were more in line with the requirements of bone regeneration than when icariin was not used (Fig. 8B), while retaining excellent porosity and achieving stable drug release (Fig. 8C). Studies in an animal model showed that the new bone mass in the functionalized 3D scaffolds increased with time (Fig. 8D). Therefore, the unique bone substitute implant promoted bone regeneration in osteonecrosis and has potential applications in clinical settings.

Ginseng has a long history of use as a Chinese herbal drug. The active ingredient of Ginseng, angiogenesis-regulating compound ginsenoside Rg1, stimulates vascularization by upregulating the expression of nitric oxide and VEGF [145]. Some researchers added ginsenoside Rg1 to poly(propylene fumarate) bone cement and showed that the functionalized 3D scaffolds exhibited appropriate drug release capacity and angiogenic ability, with potential application for accelerated bone regeneration in osteonecrosis.

3.3.2. Three-dimensional scaffolds and other drugs

Statins are commonly used clinically to reduce blood cholesterol levels. Furthermore, statins promote the expression of osteogenic genes while inhibiting adipocytic differentiation [146]. 3D scaffolds provide a local treatment pathway for statins and reduce burst release, which is conducive to the therapeutic effect of statins. Tai *et al.* [32] synthesized PLGA/HA microsphere and encapsulated simvastatin within them to generate drug-loaded functionalized 3D scaffold. After seeding with cells, the increased expression of osteogenic genes like RUNX-2 and significant mineralization supported the osteogenic effect of the functionalized 3D scaffold. After implantation of the functionalized 3D scaffolds, callus formation was found around the necrotic area of mouse tibia *in vivo*, along with neovascularization and new bone formation, indicating that bone reconstruction occurred in osteonecrosis.

Deferoxamine is an iron chelator that stimulates angiogenic gene expression and promotes the osteogenic differentiation of osteoblasts [147]. Li and co-workers used deferoxamine loaded by gelatin sponge for enhanced bone regeneration in osteonecrosis [148]. VEGF, BMP-2, and osteocalcin were up-regulated, indicating that angiogenesis and

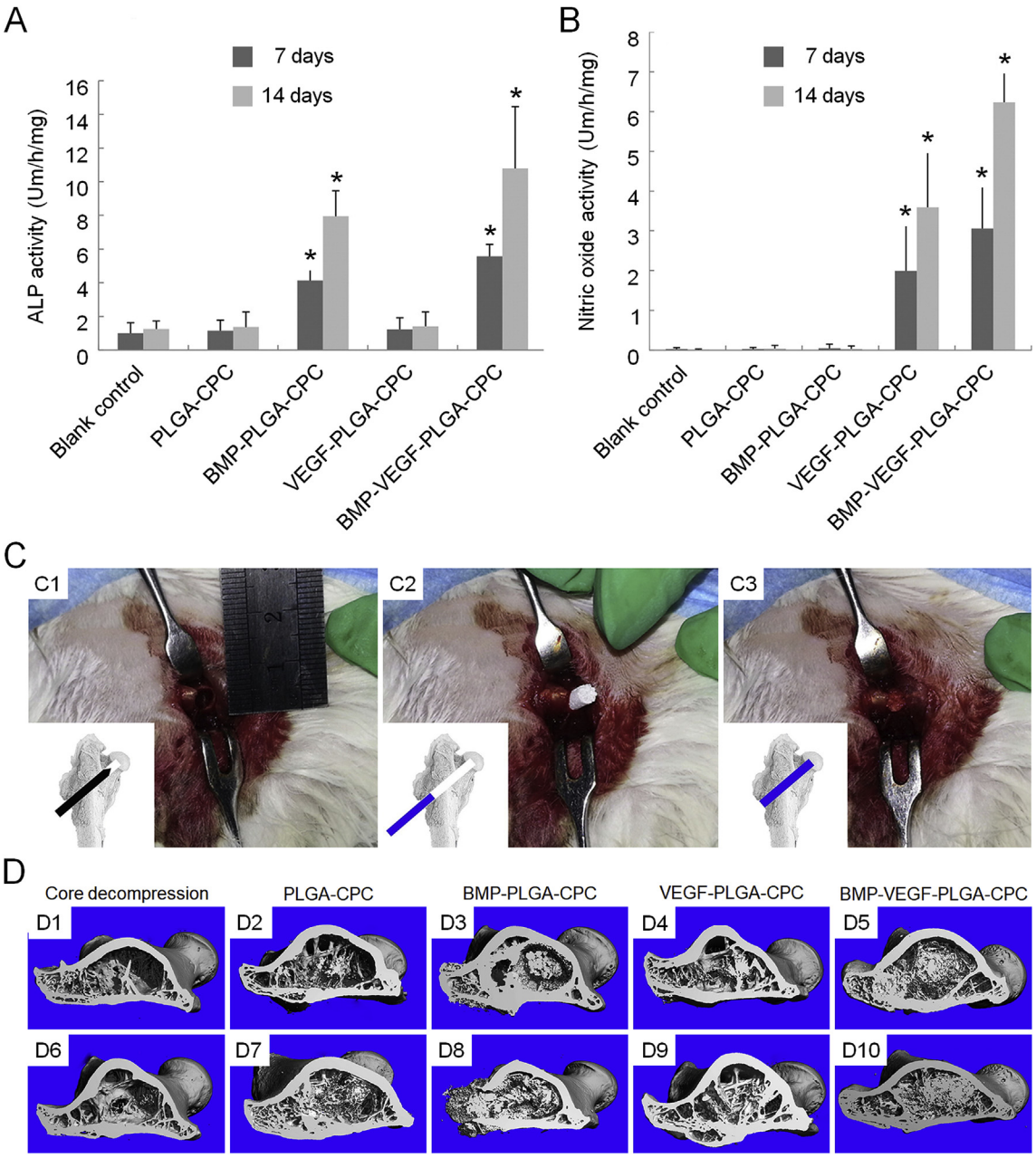

Fig. 7. BMP and VEGF dual-loaded 3D scaffolds for enhanced bone regeneration in osteonecrosis [40]. (A and B) ALP (A) and nitric oxide (B) activities in each group of BMSCs seeded after 7 and 14 days. The blank control group refers to cell culture with the cell culture plate, and the PLGA – CPC scaffold, BMP-PLGA – CPC scaffold, VEGF-PLGA – CPC scaffold, and BMP-VEGF-PLGA – CPC scaffold groups refer to cells cultured with the corresponding scaffolds. Asterisk * indicates $P < 0.05$ by Bonferroni's post-hoc tests. (C) The model of rabbits undergoing CD (C1) followed by the implantation of scaffolds into the bone defect (C2 and C3). (D) 3D reconstruction images of the femoral head by micro-CT showing newly mineralized tissue in each group in the 6^{th} week (D1 – D5) and 12^{th} week (D6 – D10). The C,D group refers to pure core decompression without implantation of scaffolds, and the PLGA – CPC scaffold, BMP-PLGA – CPC scaffold, VEGF-PLGA – CPC scaffold, and BMP-VEGF-PLGA – CPC scaffold groups refer to the implantation of the corresponding scaffolds. Reproduced with permission [40]. Copyright 2016, Elsevier Ltd.

osteogenesis were promoted. Therefore, this represented an economical and effective management option for enhanced bone regeneration in osteonecrosis. However, the mechanical performance and controlled drug release of the gelatin sponge was found to be inadequate.

3.4. Combination of three-dimensional scaffolds with metallic elements

Metallic elements play essential roles in biological processes related to health. Numerous studies have shown that the use of functionalized 3D scaffolds with composite metal elements represents a feasible strategy for accelerating bone reconstruction in osteonecrosis. Sr is a bone-seeking element with a chemical structure similar to that of calcium, which stimulates bone formation, inhibits osteoclast differentiation, and promotes angiogenesis [149–151]. Sr has been used for enhanced bone regeneration in osteonecrosis, and 3D scaffolds are one of the most effective options in this context. Sr-doped calcium polyphosphate-functionalized 3D scaffolds were revealed to be effective in repairing osteonecrotic lesions and improving angiogenesis [57].

Magnesium (Mg), which may be used as a type of metallic implantable material, exhibits excellent mechanical performance, biodegradability, and enhances bone growth and microvascular dilation [44]. However, within implants, Mg degrades rapidly *in vivo* and directly affects mechanical stability. Furthermore, a large number of by-products produced have an adverse effect on tissue healing [152]. The

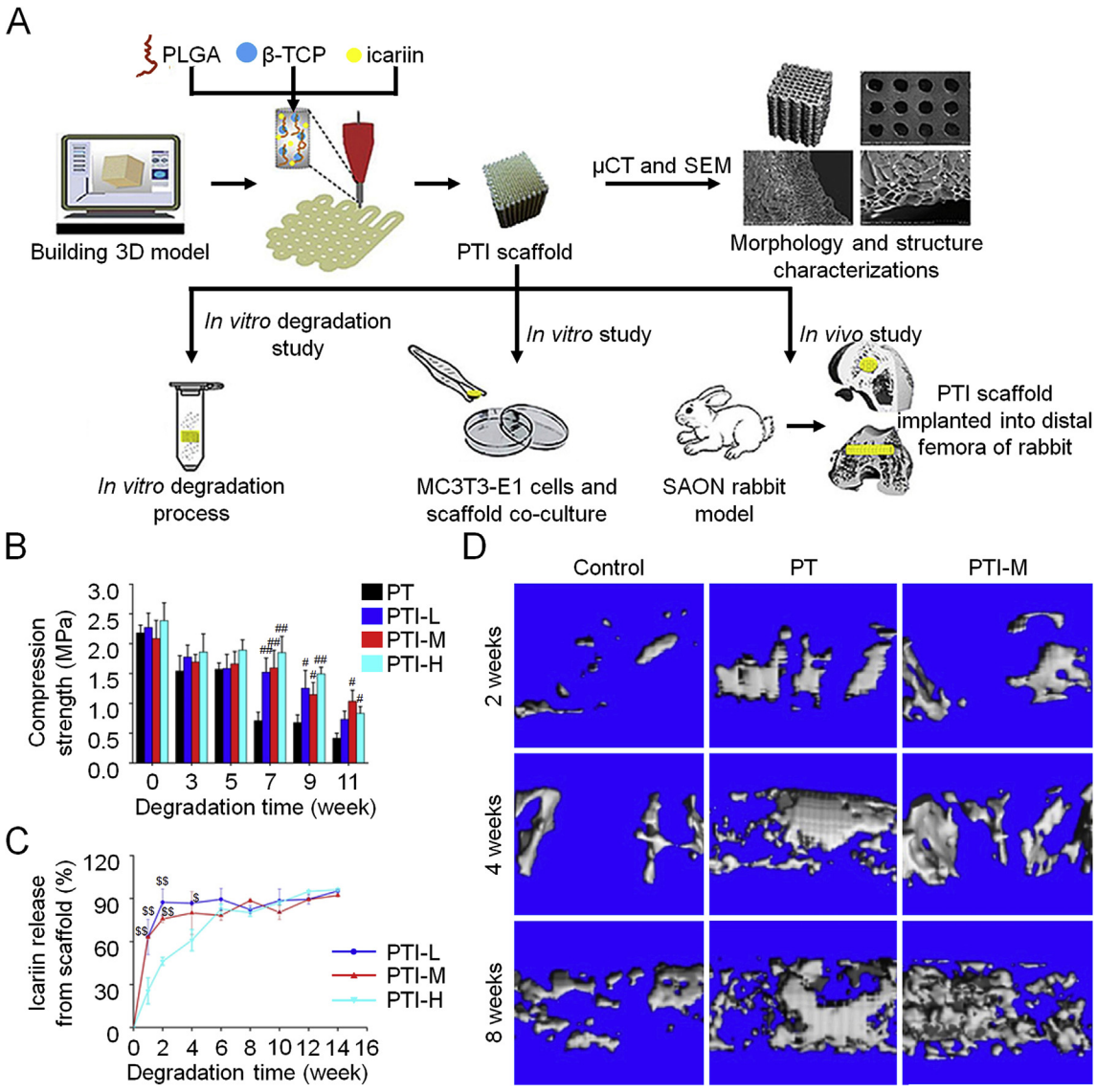

Fig. 8. Icariin-loaded 3D scaffolds for enhanced bone regeneration in osteonecrosis [39]. (A) PLGA, β-TCP, and icariin were produced into 3D scaffolds (PTI) by low-temperature 3D printing technology and used for related studies *in vivo* and *in vitro*. (B and C) Changed compressive strength of 3D scaffolds (B) and icariin released (C) during *in vitro* degradation. Superscript symbol $^{\#}$ indicates $P < 0.05$ and superscript symbol $^{\#\#}$ indicates $P < 0.01$ by Bonferroni post-test. The PT group denotes only scaffolds, and PTI-L, PTI-M, and PTI-H denote scaffolds with icariin concentrations of 0.16%, 0.32%, and 0.64%, respectively. Superscript symbol $^{\$}$ indicates $P < 0.05$ and superscript symbol $^{\$\$}$ indicates $P < 0.01$ compared with the PTI-H groups by Bonferroni post-test. (D) 3D reconstruction images of the distal femora showed the new bone formation in the defect at 2, 4, and 8 weeks after CD. Control refers to CD without implantation, and PT and PTI-M refer to CD with PT scaffolds and PTI-M scaffolds implanted. Reproduced with permission [39]. Copyright 2018, Elsevier Ltd.

application of Mg as a component of 3D scaffolds is a common strategy to resolve these limitations. Lai *et al.* [44] applied the low-temperature rapid prototyping technology to successfully integrate Mg, PLGA, and TCP into a functionalized 3D scaffold. The addition of Mg significantly improved the mechanical performance of the functionalized 3D scaffolds. After 12 weeks of implantation in the rabbit femoral condyle, newly formed bone tissue and new vessel in the functionalized 3D scaffold group were observed. In particular, in the 8th week, the group of functionalized 3D scaffolds had the most significant proportion of neovasculature and the best vascular structure. These findings established that the Mg-based functionalized 3D scaffolds exhibited great potential for enhanced bone regeneration in osteonecrosis and was expected to be useful in clinical practice.

Li is also one of the metallic elements with potential utility for enhancing bone regeneration in osteonecrosis, owing to its ability to enhance bone formation, promote vascularization, and inhibit adipogenesis, and enable rapid tissue repair through the mediation of 3D scaffolds [153–155]. Li *et al.* [59,60] established a functionalized 3D LinHA scaffold and confirmed that it improved bone formation and inhibited lipogenesis. The functionalized 3D scaffolds achieved the sustained release of Li and enhanced healing ability. The 3D scaffold containing Li enhanced bone regeneration in osteonecrosis more effectively than others (Fig. 9).

Bioactive factors were loaded onto 3D scaffolds to reduce the loss of activity before use and minimize enzymatic degradation during treatment. Furthermore, their controlled and stable release enhanced biosafety and reduced toxicity [156,157]. Therefore, the use of 3D scaffolds as mediators to enhance the effectiveness of bioactive factors and application of various strategies in combination to functionalize 3D scaffolds are of great significance for enhancing bone reconstruction in osteonecrosis.

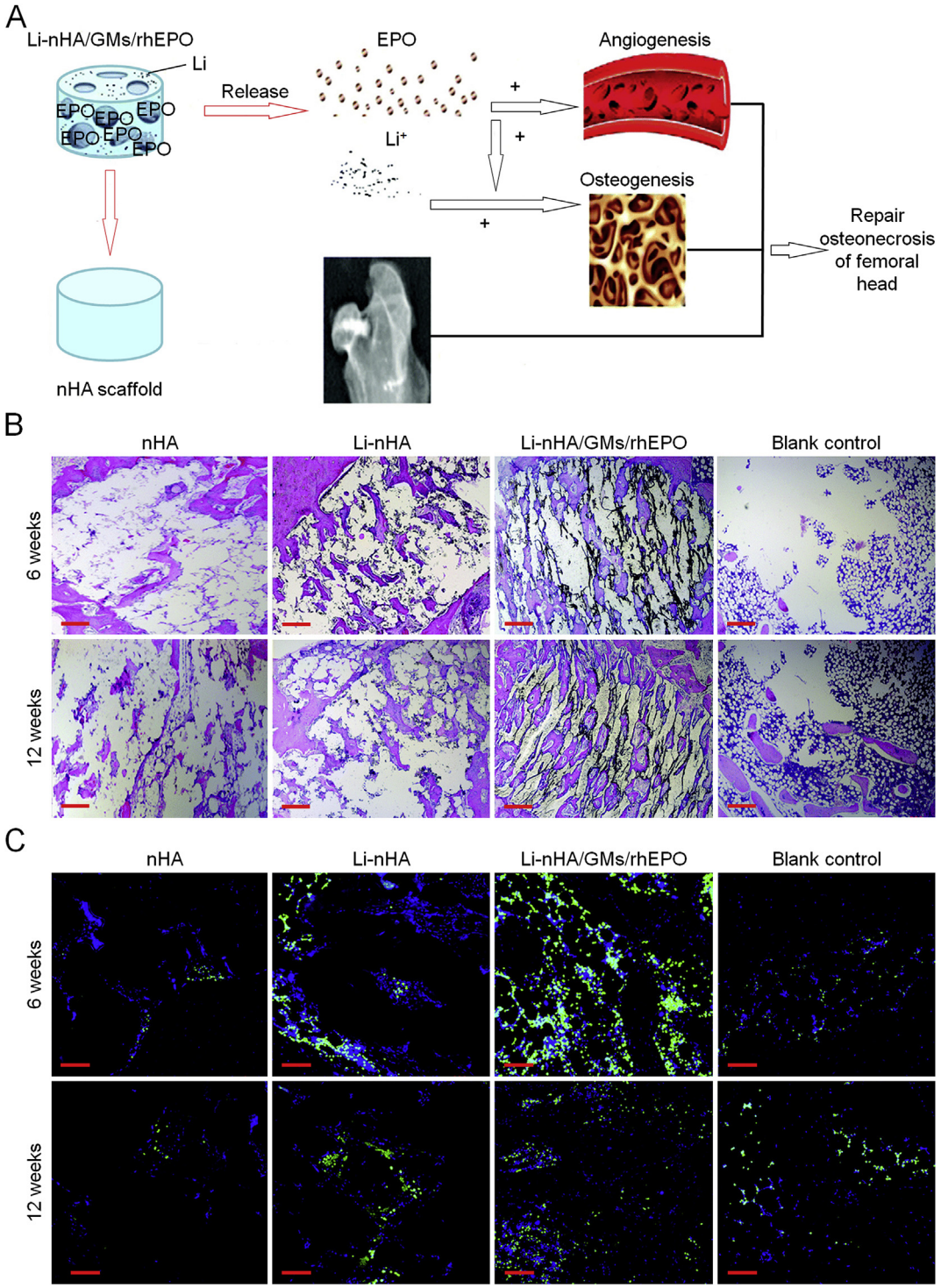

Fig. 9. Combination of 3D scaffolds with Li and EPO for enhanced bone regeneration in osteonecrosis [59]. (A) Schematic of study design. (B) H&E staining images showed the bone repair at 6 and 12 weeks. Scale bar = 200 μm. (C) At 6 and 12 weeks after surgery, immunohistochemical staining of angiogenic factor VEGF (green) took place. The blank control group refers to creating the femoral head defect without implantation, and the nHA, Li-nHA, and Li-nHA/GMs/rhEPO groups refer to repairing the femoral head defect with the implantation of corresponding 3D scaffolds. Scale bar = 100 μm. Reproduced with permission [59]. Copyright 2018, Royal Society of Chemistry.

4. Conclusions and future perspectives

Joints are sites of predilection for osteonecrosis, once the excessive destruction of bone is formed and bone regeneration is deficient, it will inevitably lead to insufficient support of the subchondral bone, resulting in joint collapse. Despite advances in the field of skeletal system repair, it is challenging to restore the normal physiological structure of the collapsed joint surface, owing to the unique properties of the cartilage, such as its multilayered cell structure, different extracellular matrix composition, and fibril orientation [158].

Therefore, it is critical to repair the necrotic area as early as possible during management. Engineered 3D scaffolds made of bioactive materials have effectively overcome many limitations of existing treatments, owing to their useful properties, such as biocompatibility,

biodegradability, porosity, and mechanical performance. Biocompatibility is a prerequisite for use *in vivo*. Non-biocompatible materials may cause inflammatory or allogeneic responses that eventually lead to immune reactions or tissue necrosis [159]. Biocompatible scaffolds provide a suitable microenvironment for adhesion and proliferation of cells, which is critical for bone regeneration in osteonecrosis.

3D scaffolds should accommodate long-term bone regeneration in osteonecrosis and ensure the stability of local physiological structures *via* controlled biodegradability and the maintenance of appropriate mechanical performance during degradation. In addition, biodegradability also avoids the need for re-surgery to remove materials, reducing physical discomfort and risk as well as economic loss to patients. In addition to biocompatibility and biodegradability, the porosity of the engineered 3D scaffolds facilitates the ingrowth of new bone and neovascularization. In particular, angiogenesis and ingrowth of blood vessels not only promote osseointegration but also enable treatment of the disease at its source and reduce the risk of osteonecrosis repair failure and recurrence, which is critical.

Finally, the appropriate mechanical performance of 3D scaffolds supports the articular surface to avoid collapse during the repair process and destruction of regenerated bone. However, most of the current studies have only explored the mechanical performance of 3D scaffolds *in vitro*, and the possibility of differences between the mechanical performance *in vivo* and *in vitro* should not be ignored. Therefore, subsequent research should aim to accurately elucidate the specific changes in the mechanical performance of 3D scaffolds *in vivo*. Furthermore, these characteristics have a mutually restrictive relationship. For example, excessive porosity may lead to a decrease in mechanical strength. In contrast, overly rapid degradation may lead to the accumulation of by-products, and overly slow degradation may affect the repair. Therefore, future studies on 3D scaffolds should focus on establishing a balance of these characteristics to achieve the best therapeutic effect.

Numerous pathological changes occur during the development of osteonecrosis. It is difficult to achieve adequate therapeutic effects using scaffolds alone, so the application of 3D scaffold-mediated management has become an inevitable tendency of development. D scaffolds incorporate bioactive factors to achieve targeted therapy, with maximal efficacy and reduced side effects. Through the preparation of appropriate materials, selection of optimal production technique, and use of a suitable loading strategy, desirable functionalized 3D scaffolds may be constructed and increasingly effective 3D scaffold-mediated therapies developed.

Currently known animal models of osteonecrosis fail to completely simulate the occurrence and development of human osteonecrosis, which is a considerable obstacle to the translation of basic research results to clinical practice. Future studies should focus on developing ideal animal models to enable the application of 3D scaffolds in the clinic.

In conclusion, 3D scaffolds offer hope for accelerating bone regeneration in osteonecrosis. Anticipated progress in the field includes the emergence of personalized 3D scaffolds that meet specific clinical needs of patients. We believe that such improved techniques will overcome existing challenges and enable unprecedented advances in the development of 3D scaffolds for enhanced bone regeneration in osteonecrosis.

CRediT authorship contribution statement

Tongtong Zhu: Conceptualization, Formal analysis, Writing - original draft, Visualization. **Yutao Cui:** Writing - review & editing. **Mingran Zhang:** Writing - review & editing. **Duoyi Zhao:** Writing - review & editing. **Guangyao Liu:** Supervision, Funding acquisition. **Jianxun Ding:** Writing - review & editing, Supervision.

Declaration of competing interest

The authors declare no competing financial interests.

Acknowledgments

This study was financially supported by the National Natural Science Foundation of China (Grant Nos. 51973216, 51873207, 51803006, and 51833010), the Science and Technology Development Program of Jilin Province (Grant No. 20190201068JC), the Youth Talents Promotion Project of Jilin Province (Grant No. 181909), the Youth Innovation Promotion Association of the Chinese Academy of Sciences (Grant No. 2019005), the Special Foundation for Provincial Authorities from Finance Department of Jilin Province (Grant No. 3D518V313429), and the State Key Laboratory of Advanced Technology for Materials Synthesis and Processing (Wuhan University of Technology) (Grant No. 2020-KF-5).

References

[1] Y. Assouline-Dayan, C. Chang, A. Greenspan, Y. Shoenfeld, M.E. Gershwin, Pathogenesis and natural history of osteonecrosis, Semin. Arthritis Rheum. 32 (2) (2002) 94–124.
[2] T. Kawai, Y. Shanjani, S. Fazeli, A.W. Behn, Y. Okuzu, S.B. Goodman, Y.Z.P. Yang, Customized, degradable, functionally graded scaffold for potential treatment of early stage osteonecrosis of the femoral head, J. Orthop. Res. 36 (3) (2018) 1002–1011.
[3] Z. Yang, H. Liu, D. Li, X. Xie, T. Qin, J. Ma, P. Kang, The efficacy of statins in preventing glucocorticoid-related osteonecrosis in animal models, Bone Joint Res. 5 (9) (2016) 393–402.
[4] R. Pascarella, R. Fantasia, P. Sangiovanni, A. Maresca, D. Massetti, R. Politano, S. Cerbasi, Traumatic hip fracture-dislocation: A middle-term follow up study and a proposal of new classification system of hip joint associated injury, Injury 50 (2019) S11–S20.
[5] I. Hermodsson, On the problem of trauma and aseptic osteonecrosis, Acta Radiol. 28 (3) (1947) 257–268.
[6] Z. Li, B. Yang, X.S. Weng, G. Tse, M.T.V. Chan, W.K.K. Wu, Emerging roles of microRNAs in osteonecrosis of the femoral head, Cell Proliferation 51 (1) (2018) e12405.
[7] R. Beckmann, H. Shaheen, N. Kweider, A. Ghassemi, A. Fragoulis, B. Hermanns-Sachweh, T. Pufe, M. Kadyrov, W. Drescher, Enoxaparin prevents steroid-related avascular necrosis of the femoral head, Sci. World J. (2014) 3478132014.
[8] J. Chen, W. Liu, Y. Cao, X. Zhang, Y. Guo, Y. Zhu, J. Li, J. Du, T. Jin, G. Wang, J. Wang, MMP-3 and MMP-8 single-nucleotide polymorphisms are related to alcohol-induced osteonecrosis of the femoral head in Chinese males, Oncotarget 8 (15) (2017) 25177–25188.
[9] J.P. Jones, S. Ramirez, S.B. Doty, The pathophysiologic role of fat in dysbaric osteonecrosis, Clin. Orthop. Relat. Res. 296 (1993) 256–264.
[10] S.S. Mogensen, K. Schmiegelow, K. Grell, B.K. Albertsen, P.S. Wehner, P. Kampmann, T.L. Frandsen, Hyperlipidemia is a risk factor for osteonecrosis in children and young adults with acute lymphoblastic leukemia, Haematologica 102 (5) (2017) e175–e178.
[11] M.C. Reed, C. Schiffer, S. Heales, A.B. Mehta, D.A. Hughes, Impact of sphingolipids on osteoblast and osteoclast activity in Gaucher disease, Mol. Genet. Metabol. 124 (4) (2018) 278–286.
[12] G.K. J, Z.F. C, G. Y, L.F. L, Z. L, Z. W, The influence of age, gender and treatment with steroids on the incidence of osteonecrosis of the femoral head during the management of severe acute respiratory syndrome, Bone Joint Lett. J. 96 (2) (2014) 259–262.
[13] Y.X. Chen, D.Y. Zhu, J.H. Yin, W.J. Yin, Y.L. Zhang, H. Ding, X.W. Yu, J. Mei, Y.S. Gao, C.Q. Zhang, The protective effect of PFTα on alcohol-induced osteonecrosis of the femoral head, Oncotarget 8 (59) (2017) 100691–100707.
[14] Z.F. Huang, C. Cheng, B.B. Cao, J. Wang, H. Wei, X.Z. Liu, Y. Han, S.H. Yang, X. Wang, Icariin protects against glucocorticoid-induced osteonecrosis of the femoral head in rats, Cell. Physiol. Biochem. 47 (2) (2018) 694–706.
[15] G.Y. Deng, K.R. Niu, F. Zhou, B.X. Li, Y.J. Kang, X.J. Liu, J.Q. Hu, B. Li, Q.G. Wang, C.Q. Yi, Q. Wang, Treatment of steroid-induced osteonecrosis of the femoral head using porous Se@SiO_2 nanocomposites to suppress reactive oxygen species, Sci. Rep. 7 (2017) 43914.
[16] T. Ichiseki, A. Kaneuji, Y. Ueda, S. Nakagawa, T. Mikami, K. Fukui, T. Matsumoto, Osteonecrosis development in a novel rat model characterized by a single application of oxidative stress, Arthritis Rheum. 63 (7) (2011) 2138–2141.
[17] L. Rackwitz, L. Eden, S. Reppenhagen, J.C. Reichert, F. Jakob, H. Walles, O. Pullig, R.S. Tuan, M. Rudert, U. Noth, Stem cell- and growth factor-based regenerative therapies for avascular necrosis of the femoral head, Stem Cell Res. Ther. 3 (1) (2012) 7.
[18] Z. Zhou, C. Pan, N. Wang, L. Zhou, H. Shan, Y. Gao, X. Yu, A high-fat diet aggravates osteonecrosis through a macrophage-derived IL-6 pathway, Int. Immunol. 31 (4) (2019) 263–273.

[19] Z. Li, L.L. Wang, J. Wei, L.G. Zhu, X.S. Weng, J. Jin, H. Xiao, J. Zhang, H.M. Wang, G.T. Shi, L.P. Pei, F.D. Zou, W.Q. Zhang, T.Z. Tao, X. Dong, Bone-strengthening pill (BSP) promotes bone cell and chondrocyte repair, and the clinical and experimental study of BSP in the treatment of osteonecrosis of the femoral head, Oncotarget 8 (57) (2017) 97079–97089.

[20] C.J.D. F, P.M. F, R.P. A, The extent of osteocyte death in the proximal femur of patients with osteonecrosis of the femoral head, J. Bone Joint Surg. Br. 83 (3) (2001) 419–422.

[21] L.Z. Zheng, H.J. Cao, S.H. Chen, T. Tang, W.M. Fu, L. Huang, D.H.K. Chow, Y.X. Wang, J.F. Griffith, W. He, H. Zhou, D.W. Zhao, G. Zhang, X.I. Wang, L. Qin, Blockage of Src by specific siRNA as a novel therapeutic strategy to prevent destructive repair in steroid-associated osteonecrosis in rabbits, J. Bone Miner. Res. 30 (11) (2015) 2044–2057.

[22] Y. Wang, X.B. Ma, W. Chai, J. Tian, Multiscale stem cell technologies for osteonecrosis of the femoral head, Stem Cell. Int. (2019) 89145692019.

[23] J.S. Kang, Y.J. Suh, K.H. Moon, J.S. Park, T.H. Roh, M.H. Park, D.J. Ryu, Clinical efficiency of bone marrow mesenchymal stem cell implantation for osteonecrosis of the femoral head: A matched pair control study with simple core decompression, Stem Cell Res. Ther. 9 (1) (2018) 274.

[24] N.S. Piuzzi, J. Chahla, J.B. Schrock, R.F. LaPrade, C. Pascual-Garrido, M.A. Mont, G.F. Muschler, Evidence for the use of cell-based therapy for the treatment of osteonecrosis of the femoral head: A systematic review of the literature, J. Arthroplasty 32 (5) (2017) 1698–1708.

[25] W.X. Peng, L. Wang, Adenovirus-mediated expression of BMP-2 and BFGF in bone marrow mesenchymal stem cells combined with demineralized bone matrix for repair of femoral head osteonecrosis in beagle dogs, Cell. Physiol. Biochem. 43 (4) (2017) 1648–1662.

[26] F. Yang, F. Xue, J.J. Guan, Z. Zhang, J.M. Yin, Q.L. Kang, Stromal cell-derived factor (SDF) 1-α overexpression promotes bone regeneration by osteogenesis and angiogenesis in osteonecrosis of the femoral head, Cell. Physiol. Biochem. 46 (6) (2018) 2561–2575.

[27] C.H. Zhou, J.H. Meng, C.C. Zhao, C.Y. Ye, H.X. Zhu, B. Hu, B.C. Heng, Y. Shen, T. Lin, X.B. Yang, Z.L. Shi, W.L. Shen, S.G. Yan, PTH 1-34 improves the effects of core decompression in early-stage steroid-associated osteonecrosis model by enhancing bone repair and revascularization, PloS One 12 (5) (2017) e0178781.

[28] H. Bakhshi, M.R. Rasouli, J. Parvizi, Can local Erythropoietin administration enhance bone regeneration in osteonecrosis of femoral head? Med. Hypotheses 79 (2) (2012) 154–156.

[29] P.P. Guo, F.Q. Gao, Y.H. Wang, Z.K. Zhang, W. Sun, B.G. Jiang, B.L. Wang, Z.R. Li, The use of anticoagulants for prevention and treatment of osteonecrosis of the femoral head: A systematic review, Medicine 96 (16) (2017) e6646.

[30] Z.H. Feng, W.H. Zheng, Q. Tang, L. Cheng, H. Li, W.F. Ni, X.Y. Pan, Fludarabine inhibits STAT1-mediated up-regulation of caspase-3 expression in dexamethasone-induced osteoblasts apoptosis and slows the progression of steroid-induced avascular necrosis of the femoral head in rats, Apoptosis 22 (8) (2017) 1001–1012.

[31] Y. Li, J. Duan, T. Guo, W. Xie, S. Yan, B. Li, Y. Zhou, Y. Chen, *In vivo* pharmacokinetics comparisons of icariin, emodin and psoralen from Gan-kang granules and extracts of Herba Epimedii, Nepal dock root, Ficus hirta yahl, J. Ethnopharmacol. 124 (3) (2009) 522–529.

[32] I.C. Tai, Y.C. Fu, C.K. Wang, J.K. Chang, M.L. Ho, Local delivery of controlled-release simvastatin/PLGA/HAp microspheres enhances bone repair, Int. J. Nanomed. 8 (2013) 3895–3904.

[33] M.C. Phipps, F. Monte, M. Mehta, H.K.W. Kim, Intraosseous delivery of bone morphogenic protein-2 using a self-assembling peptide hydrogel, Biomacromolecules 17 (7) (2016) 2329–2336.

[34] Y. Liu, B. Kuang, B.B. Rothrauff, R.S. Tuan, H. Lin, Robust bone regeneration through endochondral ossification of human mesenchymal stem cells within their own extracellular matrix, Biomaterials 218 (2019) 119336.

[35] R. Dimitriou, E. Jones, D. McGonagle, P.V. Giannoudis, Bone regeneration: Current concepts and future directions, BMC Med. 9 (1) (2011) 66.

[36] J.E. Song, N. Tripathy, D.H. Lee, J.H. Park, G. Khang, Quercetin inlaid silk fibroin/hydroxyapatite scaffold promotes enhanced osteogenesis, ACS Appl. Mater. Interfaces 10 (39) (2018) 32955–32964.

[37] L.H. Wang, Y.Y. Qiu, H.J. Lv, Y. Si, L.F. Liu, Q. Zhang, J.P. Cao, J.Y. Yu, X.R. Li, B. Ding, 3D superelastic scaffolds constructed from flexible inorganic nanofibers with self-fitting capability and tailorable gradient for bone regeneration, Adv. Funct. Mater. 29 (31) (2019) 1901407.

[38] B. Liu, F. Yang, X. Wei, X. Zhang, Y. Zhang, B. Wang, G. Liu, H. Xie, J. Yang, W. Wang, K. Qin, D. Zhao, An exploratory study of articular cartilage and subchondral bone reconstruction with bone marrow mesenchymal stem cells combined with porous tantalum/Bio-Gide® collagen membrane in osteonecrosis of the femoral head, Mater. Sci. Eng., C 99 (2019) 1123–1132.

[39] Y.X. Lai, H.J. Cao, X.L. Wang, S.K. Chen, M. Zhang, N. Wang, Z.H. Yao, Y. Dai, X.H. Xie, P. Zhang, X.S. Yao, L. Qin, Porous composite scaffold incorporating osteogenic phytomolecule icariin for promoting skeletal regeneration in challenging osteonecrotic bone in rabbits, Biomaterials 153 (2018) 1–13.

[40] H.X. Zhang, X.P. Zhang, G.Y. Xiao, Y. Hou, L. Cheng, M. Si, S.S. Wang, Y.H. Li, L. Nie, *In vitro* and *in vivo* evaluation of calcium phosphate composite scaffolds containing BMP-VEGF loaded PLGA microspheres for the treatment of avascular necrosis of the femoral head, Mater. Sci. Eng., C 60 (2016) 298–307.

[41] T. Ahmad, H.J. Shin, J. Lee, Y.M. Shin, S.K.M. Perikamana, S.Y. Park, H.S. Jung, H. Shin, Fabrication of *in vitro* 3D mineralized tissue by fusion of composite spheroids incorporating biomineral-coated nanofibers and human adipose-derived stem cells, Acta Biomater. 74 (2018) 464–477.

[42] B.M. Baker, C.S. Chen, Deconstructing the third dimension — how 3D culture microenvironments alter cellular cues, J. Cell Sci. 125 (13) (2012) 3015–3024.

[43] L. Zhang, G.J. Yang, B.N. Johnson, X.F. Jia, Three-dimensional (3D) printed scaffold and material selection for bone repair, Acta Biomater. 84 (2019) 16–33.

[44] Y. Lai, Y. Li, H. Cao, J. Long, X. Wang, L. Li, C. Li, Q. Jia, B. Teng, T. Tang, J. Peng, D. Eglin, M. Alini, D.W. Grijpma, G. Richards, L. Qin, Osteogenic magnesium incorporated into PLGA/TCP porous scaffold by 3D printing for repairing challenging bone defect, Biomaterials 197 (2019) 207–219.

[45] H.X. Liao, Z.X. Zhong, Z.L. Liu, L.P. Li, Z.M. Ling, X.N. Zou, Bone mesenchymal stem cells co-expressing VEGF and BMP-6 genes to combat avascular necrosis of the femoral head, Exp. Ther. Med. 15 (1) (2018) 954–962.

[46] C.K. Wang, M.L. Ho, G.J. Wang, J.K. Chang, C.H. Chen, Y.C. Fu, H.H. Fu, Controlled-release of rhBMP-2 carriers in the regeneration of osteonecrotic bone, Biomaterials 30 (25) (2009) 4178–4186.

[47] P.D. Fisher, G. Venugopal, T.A. Milbrandt, J.Z. Hilt, D.A. Puleo, Hydroxyapatite-reinforced *in situ* forming PLGA systems for intraosseous injection, J. Biomed. Mater. Res. 103 (7) (2015) 2365–2373.

[48] M. Maruyama, A. Nabeshima, C.C. Pan, A.W. Behn, T. Thio, T. Lin, J. Pajarinen, T. Kawai, M. Takagi, S.B. Goodman, Y.P. Yang, The effects of a functionally-graded scaffold and bone marrow-derived mononuclear cells on steroid-induced femoral head osteonecrosis, Biomaterials 187 (2018) 39–46.

[49] P. Wang, G. Li, W. Qin, B. Shi, F.J. Liu, L.L. Wang, B.N. Zhao, T.F. Sun, L. Lin, D.D. Wang, Repair of osteonecrosis of the femoral head: 3D printed Cervi cornus Colla deproteinized bone scaffolds, Orthopä 48 (3) (2019) 213–223.

[50] D. Chen, C.X. Zhang, H.J. Huo, C.C. Ji, M. Sun, L. Nie, Injectable temperature-sensitive hydrogel with VEGF loaded microspheres for vascularization and bone regeneration of femoral head necrosis, Mater. Lett. 229 (2018) 138–141.

[51] D. Gyawali, P. Nair, H.K.W. Kim, J. Yang, Citrate-based biodegradable injectable hydrogel composites for orthopedic applications, Biomater. Sci. 1 (1) (2013) 52–64.

[52] S. Sakai, M. Tamura, H. Mishima, H. Kojima, T. Uemura, Bone regeneration induced by adenoviral vectors carrying *til-1/Cbfa1* genes implanted with biodegradable porous materials in animal models of osteonecrosis of the femoral head, J. Tissue Eng. Regener. Med. 2 (2–3) (2008) 164–167.

[53] M. Salarian, W.Z. Xu, R. Bohay, E.M.K. Lui, P.A. Charpentier, Angiogenic Rg_1/Sr-doped TiO_2 nanowire/poly(propylene fumarate) bone cement composites, Macromol. Biosci. 17 (2) (2017) 1600156.

[54] Y. Wang, W. Zhu, K. Xiao, Z. Li, Q. Ma, W. Li, S. Shen, X. Weng, Self-healing and injectable hybrid hydrogel for bone regeneration of femoral head necrosis and defect, Biochem. Biophys. Res. Commun. 508 (1) (2019) 25–30.

[55] M. Berruto, M. Delcogliano, F. de Caro, G. Carimati, F. Uboldi, P. Ferrua, G. Ziveri, C.F. De Biase, Treatment of large knee osteochondral lesions with a biomimetic scaffold results of a multicenter study of 49 patients at 2-year follow-up, Am. J. Sports Med. 42 (7) (2014) 1607–1617.

[56] F. Zhang, W.X. Peng, L. Wang, J. Zhang, W.T. Dong, J.H. Wu, H. Zhang, J.B. Wang, Y. Zhao, Role of FGF-2 transfected bone marrow Mesenchymal stem cells in engineered bone tissue for repair of avascular necrosis of femoral head in rabbits, Cell. Physiol. Biochem. 48 (2) (2018) 773–784.

[57] P.D. Kang, X.W. Xie, Z. Tan, J. Yang, B. Shen, Z.K. Zhou, F.X. Pei, Repairing defect and preventing collapse of femoral head in a steroid-induced osteonecrotic of femoral head animal model using strontium-doped calcium polyphosphate combined BM-MNCs, J. Mater. Sci. Mater. Med. 26 (2) (2015) 80.

[58] G. Wang, Y. Li, T. Sun, C. Wang, L. Qiao, Y. Wang, K. Dong, T. Yuan, J. Chen, G. Chen, S. Sun, BMSC affinity peptide-functionalized β-tricalcium phosphate scaffolds promoting repair of osteonecrosis of the femoral head, J. Orthop. Surg. Res. 14 (1) (2019) 204.

[59] D.H. Li, X.W. Xie, Z.Y. Yang, C.D. Wang, Z. Wei, P.D. Kang, Enhanced bone defect repairing effects in glucocorticoid-induced osteonecrosis of the femoral head using a porous nano-lithium-hydroxyapatite/gelatin microsphere/erythropoietin composite scaffold, Biomater. Sci. 6 (3) (2018) 519–537.

[60] D.H. Li, H.F. Liu, Z.H. Jinhai, Y.Y. Zhouyuan, X.W. Xiaowei, Z. Wei, L.Z. Dongzhe, K.D. Pengde, Porous lithium-doped hydroxyapatite scaffold seeded with hypoxia-preconditioned bone-marrow mesenchymal stem cells for bonetissue regeneration, Biomed. Mater. 13 (5) (2018) 055002.

[61] Y.S. Liu, S.B. Liu, X.Y. Su, Core decompression and implantation of bone marrow mononuclear cells with porous hydroxylapatite composite filler for the treatment of osteonecrosis of the femoral head, Arch. Orthop. Trauma Surg. 133 (1) (2013) 125–133.

[62] A.D. de Almeida, F.G. Leite, M.V. Chaud, M.D. Rebelo, L. Borges, F.J.M. Viroel, A. Hataka, D. Grotto, Safety and efficacy of hydroxyapatite scaffold in the prevention of jaw osteonecrosis *in vivo*, J. Biomed. Mater. Res., Part B 106 (5) (2018) 1799–1808.

[63] W.X. Peng, L. Wang, J. Deng, Y.K. Gong, S.H. Li, Y.Y. Hu, Application of BCBB/BMP/bFGF complex in repairing femoral head necrosis in rabbit models, J. Hard Tissue Biol. 24 (1) (2015) 85–89.

[64] W.G. Bian, D.C. Li, Q. Lian, W.J. Zhang, L.Z. Zhu, X. Li, Z.M. Jin, Design and fabrication of a novel porous implant with pre-set channels based on ceramic stereolithography for vascular implantation, Biofabrication 3 (3) (2011) 034103.

[65] P. Yang, C. Bian, X. Huang, A. Shi, C. Wang, K. Wang, Core decompression in combination with nano-hydroxyapatite/polyamide 66 rod for the treatment of osteonecrosis of the femoral head, Arch. Orthop. Trauma Surg. 134 (1) (2014) 103–112.

[66] W. Zhu, Y. Zhao, Q. Ma, Y.J. Wang, Z.H. Wu, X.S. Weng, 3D-printed porous titanium changed femoral head repair growth patterns: Osteogenesis and vascularisation in porous titanium, J. Mater. Sci. Mater. Med. 28 (4) (2017) 62.

[67] D.F. Williams, On the mechanisms of biocompatibility, Biomaterials 29 (20) (2008) 2941–2953.

[68] T.H. Qazi, R. Rai, A.R. Boccaccini, Tissue engineering of electrically responsive

tissues using polyaniline based polymers: A review, Biomaterials 35 (33) (2014) 9068–9086.
[69] S. Kargozar, F. Baino, S. Hamzehlou, R.G. Hill, M. Mozafari, Bioactive glasses: Sprouting angiogenesis in tissue engineering, Trends Biotechnol. 36 (4) (2018) 430–444.
[70] K.T. Suh, S.W. Kim, H.L. Roh, M.S. Youn, J.S. Jung, Decreased osteogenic differentiation of mesenchymal stem cells in alcohol-induced osteonecrosis, Clin. Orthop. Relat. Res. 431 (2005) 220–225.
[71] R.S. Weinstein, R.L. Jilka, A.M. Parfitt, S.C. Manolagas, Inhibition of osteoblastogenesis and promotion of apoptosis of osteoblasts and osteocytes by glucocorticoids. Potential mechanisms of their deleterious effects on bone, J. Clin. Invest. 102 (2) (1998) 274–282.
[72] Y. Wang, X. Yang, Z. Gu, H. Qin, L. Li, J. Liu, X. Yu, *In vitro* study on the degradation of lithium-doped hydroxyapatite for bone tissue engineering scaffold, Mater. Sci. Eng., C 66 (2016) 185–192.
[73] X.H. Xie, X.L. Wang, G. Zhang, Y.X. He, Y. Leng, T.T. Tang, X.H. Pan, L. Qin, Biofabrication of a PLGA-TCP-based porous bioactive bone substitute with sustained release of icaritin, J. Tissue Eng. Regener. Med. 9 (8) (2015) 961–972.
[74] M. Doblaré, J.M. García, M.J. Gómez, Modelling bone tissue fracture and healing: A review, Eng. Fract. Mech. 71 (13) (2004) 1809–1840.
[75] E.S. Sanzana, M. Navarro, M.P. Ginebra, J.A. Planell, A.C. Ojeda, H.A. Montecinos, Role of porosity and pore architecture in the *in vivo* bone regeneration capacity of biodegradable glass scaffolds, J. Biomed. Mater. Res. 102 (6) (2014) 1767–1773.
[76] X. Wang, S. Xu, S. Zhou, W. Xu, M. Leary, P. Choong, M. Qian, M. Brandt, Y.M. Xie, Topological design and additive manufacturing of porous metals for bone scaffolds and orthopaedic implants: A review, Biomaterials 83 (2016) 127–141.
[77] B. Dhandayuthapani, Y. Yoshida, T. Maekawa, D.S. Kumar, Polymeric scaffolds in tissue engineering application: A review, Int. J. Polym. Sci. (2011) 2906022011.
[78] V. Karageorgiou, D. Kaplan, Porosity of 3D biomaterial scaffolds and osteogenesis, Biomaterials 26 (27) (2005) 5474–5491.
[79] J. Rnjak-Kovacina, L.S. Wray, J.M. Golinski, D.L. Kaplan, Arrayed hollow channels in silk-based scaffolds provide functional outcomes for engineering critically sized tissue constructs, Adv. Funct. Mater. 24 (15) (2014) 2188–2196.
[80] C. Feng, W.J. Zhang, C.J. Deng, G.L. Li, J. Chang, Z.Y. Zhang, X.Q. Jiang, C.T. Wu, 3D printing of lotus root-like biomimetic materials for cell delivery and tissue regeneration, Adv. Sci. 4 (12) (2017) 1700401.
[81] X. Wang, M. Lin, Y. Kang, Engineering porous β-tricalcium phosphate (β-TCP) scaffolds with multiple channels to promote cell migration, proliferation, and angiogenesis, ACS Appl. Mater. Interfaces 11 (9) (2019) 9223–9232.
[82] N. Nagarajan, A. Dupret-Bories, E. Karabulut, P. Zorlutuna, N.E. Vrana, Enabling personalized implant and controllable biosystem development through 3D printing, Biotechnol. Adv. 36 (2) (2018) 521–533.
[83] X. Wang, M. Jiang, Z. Zhou, J. Gou, D. Hui, 3D printing of polymer matrix composites: A review and prospective, Composites Part B 110 (2017) 442–458.
[84] D.W. Sommerfeldt, C.T. Rubin, Biology of bone and how it orchestrates the form and function of the skeleton, Eur. Spine J. 10 (2001) S86–S95.
[85] A.G. Guex, J.L. Puetzer, A. Armgarth, E. Littmann, E. Stavrinidou, E.P. Giannelis, G.G. Malliaras, M.M. Stevens, Highly porous scaffolds of PEDOT:PSS for bone tissue engineering, Acta Biomater. 62 (2017) 91–101.
[86] T.T. Niinimaki, P. Ohtonen, A.H. Harila-Saari, R.A. Niinimaki, Young patients with hematologic and lymphatic malignancies have an increased risk of hip and knee arthroplasty, Acta Oncol. 55 (5) (2016) 567–571.
[87] M.A. Mont, K.M. Baumgarten, A. Rifai, D.A. Bluemke, L.C. Jones, D.S. Hungerford, Atraumatic osteonecrosis of the knee, J. Bone Joint Surg. 82 (9) (2000) 1279–1290.
[88] M.A. Mont, L.C. Jones, D.S. Hungerford, Nontraumatic osteonecrosis of the femoral head: Ten years later, J. Bone Joint Surg. 88 (5) (2006) 1117–1132.
[89] Q. Mao, W.D. Wang, T.T. Xu, S.X. Zhang, L.W. Xiao, D. Chen, H.T. Jin, P.J. Tong, Combination treatment of biomechanical support and targeted intra-arterial infusion of peripheral blood stem cells mobilized by granulocyte-colony stimulating factor for the osteonecrosis of the femoral head: A randomized controlled clinical trial, J. Bone Miner. Res. 30 (4) (2015) 647–656.
[90] K. Tilkeridis, P. Touzopoulos, A. Ververidis, S. Christodoulou, K. Kazakos, G.I. Drosos, Use of demineralized bone matrix in spinal fusion, World J. Orthoped. 5 (1) (2014) 30–37.
[91] Y. Ma, N. Hu, J. Liu, X. Zhai, M. Wu, C. Hu, L. Li, Y. Lai, H. Pan, W.W. Lu, X. Zhang, Y. Luo, C. Ruan, Three-dimensional printing of biodegradable piperazine-based polyurethane-urea scaffolds with enhanced osteogenesis for bone regeneration, ACS Appl. Mater. Interfaces 11 (9) (2019) 9415–9424.
[92] I.E. Carlström, A. Rashad, E. Campodoni, M. Sandri, K. Syverud, A.I. Bolstad, K. Mustafa, Cross-linked gelatin-nanocellulose scaffolds for bone tissue engineering, Mater. Lett. 264 (2020) 127326.
[93] Z.K. Cui, S. Kim, J.J. Baljon, B.M. Wu, T. Aghaloo, M. Lee, Microporous methacrylated glycol chitosan-montmorillonite nanocomposite hydrogel for bone tissue engineering, Nat. Commun. 10 (1) (2019) 3523.
[94] L. Qin, G. Zhang, H. Sheng, K.W. Yeung, H.Y. Yeung, C.W. Chan, W.H. Cheung, J. Griffith, K.H. Chiu, K.S. Leung, Multiple bioimaging modalities in evaluation of an experimental osteonecrosis induced by a combination of lipopolysaccharide and methylprednisolone, Bone 39 (4) (2006) 863–871.
[95] L.H. Fan, C. Zhang, Z.F. Yu, Z.B. Shi, X.Q. Dang, K.Z. Wang, Transplantation of hypoxia preconditioned bone marrow mesenchymal stem cells enhances angiogenesis and osteogenesis in rabbit femoral head osteonecrosis, Bone 81 (2015) 544–553.
[96] G. Motomura, T. Yamamoto, T. Irisa, K. Miyanishi, K. Nishida, Y. Iwamoto, Dose effects of corticosteroids on the development of osteonecrosis in rabbits, J. Rheumatol. 35 (12) (2008) 2395–2399.
[97] Q. Wen, L. Ma, Y.P. Chen, L. Yang, W. Luo, X.N. Wang, A rabbit model of hormone-induced early avascular necrosis of the femoral head, Biomed. Environ. Sci. 21 (5) (2008) 398–403.
[98] X.L. Zhang, Y.M. Wang, K. Chu, Z.H. Wang, Y.H. Liu, L.H. Jiang, X. Chen, Z.Y. Zhou, G. Yin, The application of PRP combined with TCP in repairing avascular necrosis of the femoral head after femoral neck fracture in rabbit, Eur. Rev. Med. Pharmacol. Sci. 22 (4) (2018) 903–909.
[99] S.H. Chen, L.Z. Zheng, J.Y. Zhang, H. Wu, N. Wang, W.X. Tong, J.K. Xu, L. Huang, Y.F. Zhang, Z.J. Yang, G. Lin, X.L. Wang, L. Qin, A novel bone targeting delivery system carrying phytomolecule icaritin for prevention of steroid-associated osteonecrosis in rats, Bone 106 (2018) 52–60.
[100] G.Y. Deng, C.Y. Dai, J.Y. Chen, A.Q. Ji, J.P. Zhao, Y. Zhai, Y.J. Kang, X.J. Liu, Y. Wang, Q.G. Wang, Porous Se@SiO_2 nanocomposites protect the femoral head from methylprednisolone-induced osteonecrosis, Int. J. Nanomed. 13 (2018) 1809–1818.
[101] S.C. Tao, T. Yuan, B.Y. Rui, Z.Z. Zhu, S.C. Guo, C.Q. Zhang, Exosomes derived from human platelet-rich plasma prevent apoptosis induced by glucocorticoid-associated endoplasmic reticulum stress in rat osteonecrosis of the femoral head *via* the Akt/Bad/Bcl-2 signal pathway, Theranostics 7 (3) (2017) 733–750.
[102] L. Qin, D. Yao, L.Z. Zheng, W.C. Liu, Z. Liu, M. Lei, L. Huang, X.H. Xie, X.L. Wang, Y. Chen, X.S. Yao, J. Peng, H. Gong, J.F. Griffith, Y.P. Huang, Y.P. Zheng, J.Q. Feng, Y. Liu, S.H. Chen, D.M. Xiao, D.P. Wang, J.Y. Xiong, D.Q. Pei, P. Zhang, X.H. Pan, X.H. Wang, K.M. Lee, C.Y. Cheng, Phytomolecule icaritin incorporated PLGA/TCP scaffold for steroid-associated osteonecrosis: Proof-of-concept for prevention of hip joint collapse in bipedal emus and mechanistic study in quadrupedal rabbits, Biomaterials 59 (2015) 125–143.
[103] B.D. Sui, C.H. Hu, A.Q. Liu, C.X. Zheng, K. Xuan, Y. Jin, Stem cell-based bone regeneration in diseased microenvironments: Challenges and solutions, Biomaterials 196 (2019) 18–30.
[104] P. Hernigou, C.H. Flouzat-Lachaniette, J. Delambre, A. Poignard, J. Allain, N. Chevallier, H. Rouard, Osteonecrosis repair with bone marrow cell therapies: State of the clinical art, Bone 70 (2015) 102–109.
[105] J.E. Song, J. Tian, Y.J. Kook, M. Thangavelu, J.H. Choi, G. Khang, A BMSCs-laden quercetin/duck's feet collagen/hydroxyapatite sponge for enhanced bone regeneration, J. Biomed. Mater. Res. 108 (3) (2020) 784–794.
[106] R.X. Shao, R.F. Quan, T. Wang, W.B. Du, G.Y. Jia, D. Wang, L.B. Lv, C.Y. Xu, X.C. Wei, J.F. Wang, D.S. Yang, Effects of a bone graft substitute consisting of porous gradient HA/ZrO2 and gelatin/chitosan slow-release hydrogel containing BMP-2 and BMSCs on lumbar vertebral defect repair in rhesus monkey, J. Tissue Eng. Regener. Med. 12 (3) (2018) e1813–e1825.
[107] H. P, B. F, L.J. C, Decrease in the mesenchymal stem-cell pool in the proximal femur in corticosteroid-induced osteonecrosis, J. Bone Joint Surg. Br. 81 (2) (1999) 349–355.
[108] J.A. Peng, C.Y. Wen, A.Y. Wang, Y. Wang, W.J. Xu, B. Zhao, L. Zhang, S.B. Lu, L. Qin, Q.Y. Guo, L.M. Dong, J.M. Tian, Micro-CT-based bone ceramic scaffolding and its performance after seeding with mesenchymal stem cells for repair of load-bearing bone defect in canine femoral head, J. Biomed. Mater. Res., Part B 96 (2) (2011) 316–325.
[109] B.R. Levine, S. Sporer, R.A. Poggie, C.J. Della Valle, J.J. Jacobs, Experimental and clinical performance of porous tantalum in orthopedic surgery, Biomaterials 27 (27) (2006) 4671–4681.
[110] Z. Tang, Y. Xie, F. Yang, Y. Huang, C. Wang, K. Dai, X. Zheng, X. Zhang, Porous tantalum coatings prepared by vacuum plasma spraying enhance bmscs osteogenic differentiation and bone regeneration *in vitro* and *in vivo*, PloS One 8 (6) (2013) e66263.
[111] C.C. Tsai, T.L. Yew, D.C. Yang, W.H. Huang, S.C. Hung, Benefits of hypoxic culture on bone marrow multipotent stromal cells, Am. J. Blood Res. 2 (3) (2012) 148.
[112] R.K. Sen, S.K. Tripathy, S. Aggarwal, N. Marwaha, R.R. Sharma, N. Khandelwal, Early results of core decompression and autologous bone marrow mononuclear cells instillation in femoral head osteonecrosis: A randomized control study, J. Arthroplasty 27 (5) (2012) 679–686.
[113] T. Hisatome, Y. Yasunaga, S. Yanada, Y. Tabata, Y. Ikada, M. Ochi, Neovascularization and bone regeneration by implantation of autologous bone marrow mononuclear cells, Biomaterials 26 (22) (2005) 4550–4556.
[114] T. Yamasaki, Y. Yasunaga, M. Ishikawa, T. Hamaki, M. Ochi, Bone marrow-derived mononuclear cells with a porous hydroxyapatite scaffold for the treatment of osteonecrosis of the femoral head: A preliminary study, J. Bone Joint Surg. 92 (3) (2010) 337–341.
[115] C. Epple, A. Haumer, T. Ismail, A. Lunger, A. Scherberich, D.J. Schaefer, I. Martin, Prefabrication of a large pedicled bone graft by engineering the germ for *de novo* vascularization and osteoinduction, Biomaterials 192 (2019) 118–127.
[116] V. Planat-Benard, J.S. Silvestre, B. Cousin, M. André, M. Nibbelink, R. Tamarat, M. Clergue, C. Manneville, C. Saillan-Barreau, M. Duriez, A. Tedgui, B. Levy, L. Pénicaud, L. Casteilla, Plasticity of human adiposelineage cells toward endothelial cells, Circulation 109 (5) (2004) 656–663.
[117] S. Güven, A. Mehrkens, F. Saxer, D.J. Schaefer, R. Martinetti, I. Martin, A. Scherberich, Engineering of large osteogenic grafts with rapid engraftment capacity using mesenchymal and endothelial progenitors from human adipose tissue, Biomaterials 32 (25) (2011) 5801–5809.
[118] A. Scherberich, R. Galli, C. Jaquiery, J. Farhadi, I. Martin, Three-dimensional perfusion culture of human adipose tissue-derived endothelial and osteoblastic progenitors generates osteogenic constructs with intrinsic vascularization capacity, Stem Cell. 25 (7) (2007) 1823–1829.
[119] T. Ismail, R. Osinga, A. Todorov, A. Haumer, L.A. Tchang, C. Epple, N. Allafi, N. Menzi, R.D. Largo, A. Kaempfen, I. Martin, D.J. Schaefer, A. Scherberich, Engineered, axially-vascularized osteogenic grafts from human adipose-derived

cells to treat avascular necrosis of bone in a rat model, Acta Biomater. 63 (2017) 236–245.
[120] L. Zhao, A.D. Kaye, A.J. Kaye, A. Abd-Elsayed, Stem cell therapy for osteonecrosis of the femoral head: Current trends and comprehensive review, Curr. Pain Headache Rep. 22 (6) (2018) 9.
[121] S. Zuo, Y. Gong, Application and prospects of bone marrow mesenchymal stem cells and cytokines in the treatment of femoral head necrosis, Chin. J. Tissue Eng. Res. 16 (14) (2012) 2621–2624.
[122] L.J. Shi, W. Sun, F.Q. Gao, L.M. Cheng, Z.R. Li, Heterotopic ossification related to the use of recombinant human BMP-2 in osteonecrosis of femoral head, Medicine 96 (27) (2017) 6.
[123] C. Laflamme, M. Rouabhia, Effect of BMP-2 and BMP-7 homodimers and a mixture of BMP-2/BMP-7 homodimers on osteoblast adhesion and growth following culture on a collagen scaffold, Biomed. Mater. 3 (1) (2008) 10.
[124] C. Zhao, N.T. Qazvini, M. Sadati, Z. Zeng, S. Huang, A.L. De La Lastra, L. Zhang, Y. Feng, W. Liu, B. Huang, B. Zhang, Z. Dai, Y. Shen, X. Wang, W. Luo, B. Liu, Y. Lei, Z. Ye, L. Zhao, D. Cao, L. Yang, X. Chen, A. Athiviraham, M.J. Lee, J.M. Wolf, R.R. Reid, M. Tirrell, W. Huang, J.J. de Pablo, T.C. He, A pH-triggered, self-assembled, and bioprintable hybrid hydrogel scaffold for mesenchymal stem cell based bone tissue engineering, ACS Appl. Mater. Interfaces 11 (9) (2019) 8749–8762.
[125] T.Q. Ngo, M.A. Scherer, F.H. Zhou, B.K. Foster, C.J. Xian, Expression of bone morphogenic proteins and receptors at the injured growth plate cartilage in young rats, J. Histochem. Cytochem. 54 (8) (2006) 945–954.
[126] M.M.L. Deckers, R.L. van Bezooijen, G. van der Horst, J. Hoogendam, C. van der Bent, S.E. Papapoulos, C.W.G.M. Löwik, Bone morphogenetic proteins stimulate angiogenesis through osteoblast-derived vascular endothelial growth factor A, Endocrinology 143 (4) (2002) 1545–1553.
[127] A. Hatefi, B. Amsden, Biodegradable injectable *in situ* forming drug delivery systems, J. Contr. Release 80 (1) (2002) 9–28.
[128] N. Ferrara, H.P. Gerber, J. LeCouter, The biology of VEGF and its receptors, Nat. Med. 9 (2003) 669–676.
[129] Y. Bai, Y. Leng, G. Yin, X. Pu, Z. Huang, X. Liao, X. Chen, Y. Yao, Effects of combinations of BMP-2 with FGF-2 and/or VEGF on HUVECs angiogenesis *in vitro* and CAM angiogenesis *in vivo*, Cell Tissue Res. 356 (1) (2014) 109–121.
[130] P. Garcia, A. Pieruschka, M. Klein, A. Tami, T. Histing, J.H. Holstein, C. Scheuer, T. Pohlemann, M.D. Menger, Temporal and spatial vascularization patterns of unions and nonunions: Role of vascular endothelial growth factor and bone morphogenetic proteins, J. Bone Joint Surg. 94 (1) (2012) 49–58.
[131] Y.H. Kim, H. Furuya, Y. Tabata, Enhancement of bone regeneration by dual release of a macrophage recruitment agent and platelet-rich plasma from gelatin hydrogels, Biomaterials 35 (1) (2014) 214–224.
[132] Y. Shiozawa, Y.H. Jung, A.M. Ziegler, E.A. Pedersen, J.H. Wang, Z. Wang, J.H. Song, J.C. Wang, C.H. Lee, S. Sud, K.J. Pienta, P.H. Krebsbach, R.S. Taichman, Erythropoietin couples hematopoiesis with bone formation, PloS One 5 (5) (2010) 14.
[133] J. Kim, Y.H. Jung, H.L. Sun, J. Joseph, A. Mishra, Y. Shiozawa, J.C. Wang, P.H. Krebsbach, R.S. Taichman, Erythropoietin mediated bone formation is regulated by mTOR signaling, J. Cell. Biochem. 113 (1) (2012) 220–228.
[134] R.Y. Hu, Y. Cheng, H. Jing, H.W. Wu, Erythropoietin promotes the protective properties of transplanted endothelial progenitor cells against acute lung injury *via* PI3K/Akt pathway, Shock 42 (4) (2014) 327–336.
[135] N. Koike, D. Fukumura, O. Gralla, P. Au, J.S. Schechner, R.K. Jain, Creation of long-lasting blood vessels, Nature 428 (6979) (2004) 138–139.
[136] J.Y. Zhang, K.G. Neoh, E.T. Kang, Electrical stimulation of adipose-derived mesenchymal stem cells and endothelial cells co-cultured in a conductive scaffold for potential orthopaedic applications, J. Tissue Eng. Regener. Med. 12 (4) (2018) 878–889.
[137] C.T. Laurencin, K.M. Ashe, N. Henry, H.M. Kan, K.W.H. Lo, Delivery of small molecules for bone regenerative engineering: Preclinical studies and potential clinical applications, Drug Discov. Today 19 (6) (2014) 794–800.
[138] K.W.H. Lo, K.M. Ashe, H.M. Kan, C.T. Laurencin, The role of small molecules in musculoskeletal regeneration, Regen. Med. 7 (4) (2012) 535–549.
[139] P.B. Duell, W.E. Connor, D.R. Illingworth, Rhabdomyolysis after taking atorvastatin with gemfibrozil, Am. J. Cardiol. 81 (3) (1998) 368–369.
[140] M. Laurenti, A. Lamberti, G.G. Genchi, I. Roppolo, G. Canavese, C. Vitale-Brovarone, G. Ciofani, V. Cauda, Graphene oxide finely tunes the bioactivity and drug delivery of mesoporous ZnO scaffolds, ACS Appl. Mater. Interfaces 11 (1) (2019) 449–456.
[141] H. Ma, X. He, Y. Yang, M. Li, D. Hao, Z. Jia, The genus Epimedium: An ethnopharmacological and phytochemical review, J. Ethnopharmacol. 134 (3) (2011) 519–541.
[142] L. Song, J. Zhao, X. Zhang, H. Li, Y. Zhou, Icariin induces osteoblast proliferation, differentiation and mineralization through estrogen receptor-mediated ERK and JNK signal activation, Eur. J. Pharmacol. 714 (1) (2013) 15–22.
[143] D. Yao, X.H. Xie, X.L. Wang, C. Wan, Y.W. Lee, S.H. Chen, D.Q. Pei, Y.X. Wang, G. Li, L. Qin, Icaritin, an exogenous phytomolecule, enhances osteogenesis but not angiogenesis—an *in vitro* efficacy study, PloS One 7 (8) (2012) e41264.
[144] Y.B. Tang, A. Jacobi, C. Vater, L.J. Zou, X.N. Zou, M. Stiehler, Icariin promotes angiogenic differentiation and prevents oxidative stress-induced autophagy in endothelial progenitor cells, Stem Cell. 33 (6) (2015) 1863–1877.
[145] P.Y.K. Yue, N.K. Mak, Y.K. Cheng, K.W. Leung, T.B. Ng, D.T.P. Fan, H.W. Yeung, R.N.S. Wong, Pharmacogenomics and the Yin/Yang actions of ginseng: Anti-tumor, angiomodulating and steroid-like activities of ginsenosides, Chin. Med. 2 (1) (2007) 6.
[146] C.L. Song, Z.Q. Guo, Q.J. Ma, Z.Q. Chen, Z.J. Liu, H.T. Jia, G.T. Dang, Simvastatin induces osteoblastic differentiation and inhibits adipocytic differentiation in mouse bone marrow stromal cells, Biochem. Biophys. Res. Commun. 308 (3) (2003) 458–462.
[147] Y.F. Yan, H. Chen, H.B. Zhang, C.J. Guo, K. Yang, K.Z. Chen, R.Y. Cheng, N.D. Qian, N. Sandler, Y.S. Zhang, H.K. Shen, J. Qi, W.G. Cui, L.F. Deng, Vascularized 3D printed scaffolds for promoting bone regeneration, Biomaterials 190 (2019) 97–110.
[148] J. Li, L.H. Fan, Z.F. Yu, X.Q. Dang, K.Z. Wang, The effect of deferoxamine on angiogenesis and bone repair in steroid-induced osteonecrosis of rabbit femoral heads, Exp. Biol. Med. 240 (2) (2015) 273–280.
[149] F.J. Zhao, B. Lei, X. Li, Y.F. Mo, R.X. Wang, D.F. Chen, X.F. Chen, Promoting *in vivo* early angiogenesis with sub-micrometer strontium-contained bioactive microspheres through modulating macrophage phenotypes, Biomaterials 178 (2018) 36–47.
[150] E. Bonnelye, A. Chabadel, F. Saltel, P. Jurdic, Dual effect of strontium ranelate: Stimulation of osteoblast differentiation and inhibition of osteoclast formation and resorption *in vitro*, Bone 42 (1) (2008) 129–138.
[151] P.J. Marie, P. Ammann, G. Boivin, C. Rey, Mechanisms of action and therapeutic potential of strontium in bone, Calcif. Tissue Int. 69 (3) (2001) 121–129.
[152] M. Yazdimamaghani, M. Razavi, D. Vashaee, K. Moharamzadeh, A.R. Boccaccini, L. Tayebi, Porous magnesium-based scaffolds for tissue engineering, Mater. Sci. Eng., C 71 (2017) 1253–1266.
[153] L. Li, X. Peng, Y. Qin, R. Wang, J. Tang, X. Cui, T. Wang, W. Liu, H. Pan, B. Li, Acceleration of bone regeneration by activating Wnt/β-catenin signalling pathway *via* lithium released from lithium chloride/calcium phosphate cement in osteoporosis, Sci. Rep. 7 (2017) 45204.
[154] L. Cao, W. Weng, X. Chen, J. Zhang, Q. Zhou, J. Cui, Y. Zhao, J.W. Shin, J. Su, Promotion of *in vivo* degradability, vascularization and osteogenesis of calcium sulfate-based bone cements containing nanoporous lithium doping magnesium silicate, Int. J. Nanomed. 12 (2017) 1341–1352.
[155] L. Tang, Y. Chen, F. Pei, H. Zhang, Lithium chloride modulates adipogenesis and osteogenesis of human bone marrow-derived mesenchymal stem cells, Cell. Physiol. Biochem. 37 (1) (2015) 143–152.
[156] Y. He, S. Chen, Z. Liu, C. Cheng, H. Li, M. Wang, Toxicity of selenium nanoparticles in male Sprague-Dawley rats at supranutritional and nonlethal levels, Life Sci. 115 (1) (2014) 44–51.
[157] G. Wei, G.J. Pettway, L.K. McCauley, P.X. Ma, The release profiles and bioactivity of parathyroid hormone from poly(lactic-*co*-glycolic acid) microspheres, Biomaterials 25 (2) (2004) 345–352.
[158] L. Keller, L. Pijnenburg, Y. Idoux-Gillet, F. Bornert, L. Benameur, M. Tabrizian, P. Auvray, P. Rosset, R.M. Gonzalo-Daganzo, E.G. Barrena, L. Gentile, N. Benkirane-Jessel, Preclinical safety study of a combined therapeutic bone wound dressing for osteoarticular regeneration, Nat. Commun. 10 (2019) 1–10.
[159] D.W. Hutmacher, Scaffolds in tissue engineering bone and cartilage, Biomaterials 21 (24) (2000) 2529–2543.